



#### LEGAL NOTICE

This report was prepared as an account of Government sponsored work. Neither the United States, nor the Commission, nor any person acting on behalf of the Commission:

A. Makes any warranty or representation, expressed or implied, with respect to the accuracy, completeness, or usefulness of the information contained in this report, or that the use of any information, apparatus, method, or process disclosed in this report may not infringe privately owned rights; or

B. Assumes any liabilities with respect to the use of, or for damages resulting from the use of any information, apparatus, method, or process disclosed in this report.

As used in the above, "person acting on behalf of the Commission" includes any employee or contractor of the Commission, or employee of such contractor, to the extent that such employee or contractor of the Commission, or employee of such contractor prepares, disseminates, or provides access to, any information pursuant to his employment or contract with the Commission, or his employment with such contractor.

~~CONFIDENTIAL~~

ORNL-TM-1368

Contract No. W-7405-eng-26

REACTOR DIVISION

CONTROL CONCEPTS AND DIGITAL COMPUTER ANALYSIS  
OF THE MPRE FLUID SYSTEM

M. E. LaVerne

FEB 1966

OAK RIDGE NATIONAL LABORATORY  
Oak Ridge, Tennessee  
operated by  
UNION CARBIDE CORPORATION  
for the  
U. S. ATOMIC ENERGY COMMISSION

~~CONFIDENTIAL DATA~~

This document contains information which is exempt from automatic  
downgrading and declassification under the provisions of the  
Atomic Energy Act of 1954. Its transmission or disclosure in any  
manner to unauthorized persons is prohibited.

GROUP 1

Excluded from automatic downgrading and declassification

~~CONFIDENTIAL~~

1

2  
3  
4  
5  
6  
7  
8  
9  
10  
11  
12  
13  
14  
15  
16  
17  
18  
19  
20  
21  
22  
23  
24  
25  
26  
27  
28  
29  
30  
31  
32  
33  
34  
35  
36  
37  
38  
39  
40  
41  
42  
43  
44  
45  
46  
47  
48  
49  
50  
51  
52  
53  
54  
55  
56  
57  
58  
59  
60  
61  
62  
63  
64  
65  
66  
67  
68  
69  
70  
71  
72  
73  
74  
75  
76  
77  
78  
79  
80  
81  
82  
83  
84  
85  
86  
87  
88  
89  
90  
91  
92  
93  
94  
95  
96  
97  
98  
99  
100

101

## CONTENTS

	<u>Page</u>
Introduction .....	1
Description of the MPRE System .....	2
System Control .....	5
Problem Areas .....	16
Stability of the Reactor .....	16
Boiling and Condensing Flow Stability .....	17
Stability of the Complete System .....	18
Inventory Distribution .....	19
MPRE Fluid System Analysis .....	19
Results of Computer Calculations .....	27
Conclusions .....	37
Appendix A .....	43
System Equations .....	43
Turbine Equations .....	43
Jet-Pump Equations .....	46
Boiler Equations .....	47
Boiler Jet-Pump Equations .....	49
Condenser Jet-Pump Equations .....	51
Centrifugal Pump Equations .....	53
Appendix B .....	57
Two-Phase Pressure Drop Equations .....	57
Preheating Section Pressure Drop .....	58
Boiling Section Pressure Drop .....	58
Overall Pressure Drop .....	61
References .....	63



CONTROL CONCEPTS AND DIGITAL COMPUTER  
ANALYSIS OF THE MPRE FLUID SYSTEM

M. E. LaVerne

INTRODUCTION

The difficult control problems encountered in steam plants with once-through boilers indicate that there is good reason to consider a fresh approach to the control of Rankine cycle systems when attempting to develop a simple and reliable space power plant. The single-loop Rankine cycle system of the MPRE was devised in 1958 to obtain the highest possible performance for a given reactor outlet temperature and to obtain a system sufficiently simple that the probability of its operating satisfactorily and unattended for 10,000 hours would be high.<sup>1</sup> An important feature of the system is that the fluid dynamic and thermodynamic performance characteristics of the components and the nuclear characteristics of the reactor can be integrated and matched to eliminate most of the control functions required for a conventional power plant system.

While the stability and control problems of the MPRE may be unusual, there is reason to believe that they are substantially less complex than those of a conventional system. Because of the unorthodox character of the system, these problems have been attacked from a number of different angles. Analytical work has led to the formulation of models for the Rankine cycle and these have been employed in work with both a digital computer and an analog.<sup>2</sup> Five electrically heated Rankine cycle mockups have been built and operated, two with water and three with potassium.<sup>3,4</sup> Glass and plastic parts permitted viewing of the liquid flow in the water systems.

The first portion of this report describes the basic system and outlines the manner in which it is designed to operate. The various stability and control problems are outlined to indicate their relationship and to put each in perspective. Of necessity, this portion relies

heavily on, and borrows equally heavily from, the work of others. The second portion of the report summarizes the digital computer analysis of the Rankine cycle system.

#### DESCRIPTION OF THE MPRE SYSTEM

A vertical section through the MPRE reactor is shown in Fig. 1. The reactor core consists of a bundle of 1/2-in.-diam stainless steel tubes filled with sintered pellets of fully enriched  $UO_2$ . The upper ends of these rods are filled with BeO to provide a reflector region. A separator is provided at the top of the core to remove the liquid from the vapor-liquid mixture leaving the core. Tests with air-water mixtures indicate that vapor exit qualities in excess of 99% can be obtained. Wedge-shaped flat slabs of BeO are arranged radially around the reactor core to form a 3-in.-thick reflector. Reactor control is accomplished by raising or lowering the bottom end plug, which is divided into four independently operable quadrants. This is discussed in a companion paper,<sup>5</sup> as are the reactor physics<sup>6</sup> and the heat transfer and fluid flow problems of the system.<sup>7</sup>

A schematic diagram of the system is shown in Fig. 2. Vapor flows from the vapor separator to the turbine and then to the condenser. Liquid from the condenser is returned by a jet pump to a centrifugal feed pump from which it is delivered to the reactor core circuit through a set of four jet pumps operating in parallel to recirculate the liquid from the vapor separator to the core inlet.

The centrifugal feed pump of Fig. 2 is not an integral part of the turbine-generator unit but is driven by a separate turbine. This arrangement has the advantage that it separates the development problems and has made it possible to proceed with tests on the MPRE system without a turbine-generator unit. Until a turbine-generator becomes available, it can be simulated by a bypass valve or orifice which will have essentially the same flow characteristics. Of course, vapor emerging from a valve or orifice in parallel with the free turbine-pump unit will be somewhat superheated. This superheat can be removed easily by means of a cooler

ORNL-LR-DWG 63-6045

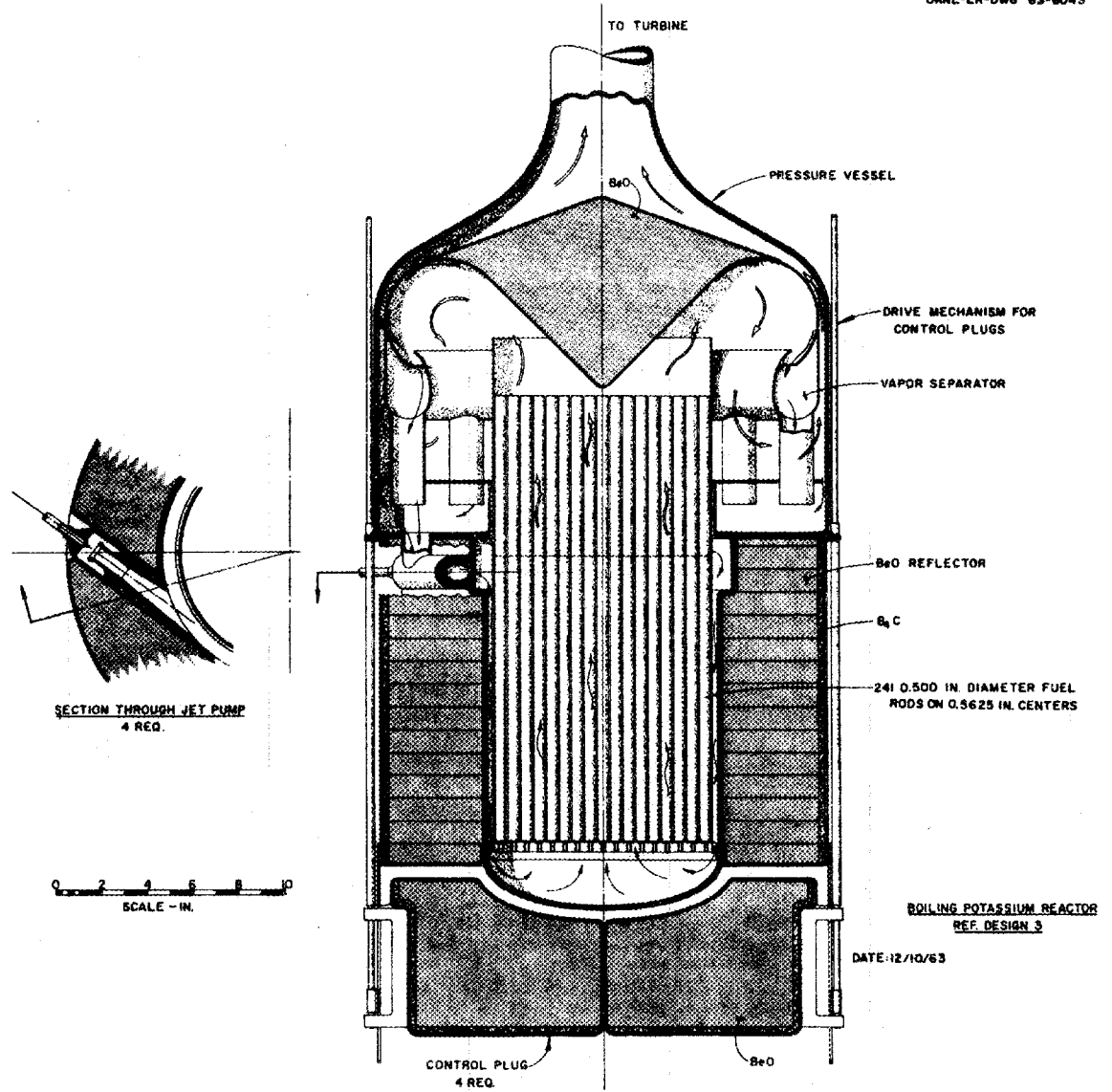


Fig. 1. Vertical Section Through the MPRE Reactor.

CONFIDENTIAL  
ORNL-DWG 65-10676

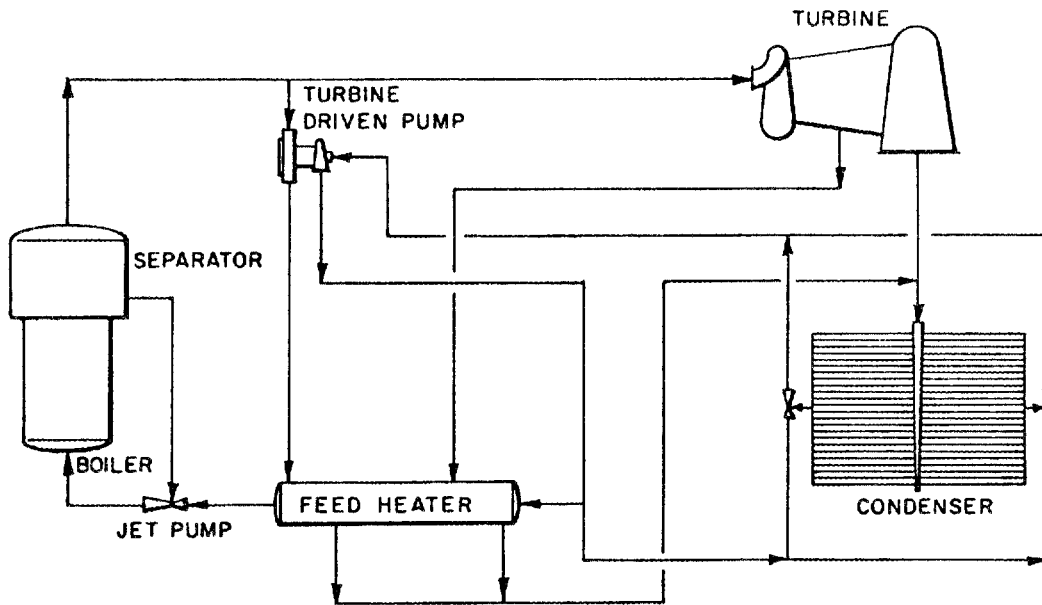


Fig. 2. Schematic Diagram of the MPRE Potassium System.

downstream of the bypass orifice in order to simulate closely the condition of the vapor leaving an actual turbine. Such a combination of orifice and cooler, or "surrogate turbine", is planned for installation in the Large Potassium System test rig. If there were no heat losses, a boiler outlet temperature of 1540°F would give a vapor temperature entering the condenser of about 1280°F. Thus, the enthalpy of superheat would run only about 40 Btu/lb as compared to the heat of vaporization of 887 Btu/lb (at 1040°F).

Separation of the pump from the turbine-generator unit has a number of additional advantages. It simplifies the design of the bearing and shaft system for the turbine and generator units and eliminates what could be an awkward temperature distribution and thermal distortion problem. It gives a much higher reliability for the pump than can be obtained with an electric motor drive which would be dependent on the reliability of many other components. Most important of all, however, it greatly eases the problems of matching the characteristics of the various components of the system and thus makes it possible to obtain a system that requires relatively little electronic control equipment. This, in turn, greatly increases the overall reliability of the complete power plant.

#### SYSTEM CONTROL

The MPRE presented a whole set of abstruse design problems of which the first and most important was to obtain a system having good dynamic stability characteristics over a wide operating range. The layout of Fig. 2 was devised in an effort to simplify the system and to minimize the number of components, including the amount of instrumentation and control equipment required. Reducing the number of components to the bare essentials makes it necessary to tailor each component so that it fits well into the system. One of the innovations in the MPRE is that, unlike conventional steam turbine systems, no throttle valve is employed. Instead, the system is intended to operate in a manner much like that of a closed-cycle gas-turbine system, with

the vapor velocities through the turbine piping and other elements of the system held substantially constant over a wide range of boiler outputs while the system pressure varies essentially in direct proportion to the load. Figure 3 shows the inherent characteristics of the system. Note that the boiler pressure is directly proportional to the heat input to the boiler.

Note, too, that the speed of the free turbine-pump unit increases gradually with boiler output, and one of the problems is to adjust the slope of this curve so that it yields a feed pump output that fits the system requirements.

It is implicit in the above discussion that the power input to the boiler and hence the weight flow of vapor through the turbine should be controlled to maintain the speed of the turbine-generator unit constant irrespective of the electrical load. If the fluid system is stable under steady-state conditions throughout the operating range--and there is substantial experience with electrically heated test rigs to indicate that it is--the question then becomes one of the effects on the potassium vapor system of deviations in turbine-generator speed from the desired values.

In turbines of the type that will be used, the pressure ratio across the turbine is roughly ten times the critical ratio. As a consequence, the vapor flow through the turbine will behave essentially as though it were passing through a critical pressure drop orifice, and the turbine rotor speed will have virtually no effect on the vapor flow rate (see Fig. 4). The speed of the turbine-generator unit should be held constant to maintain the voltage and frequency; however, if something prevents this, the turbine speed may vary over a wide range with no adverse effects on the flow through the reactor.

The quality of the mixture leaving the turbine will, of course, change with the amount of work removed from the vapor. For either a stalled rotor or a complete runaway condition, the turbine would act as a throttling device; no work would be removed from the vapor, so that, as pointed out above, it would enter the condenser superheated. In practice, the extent of the turbine speed variation should be very much less - perhaps 10% - hence, the change in vapor quality will

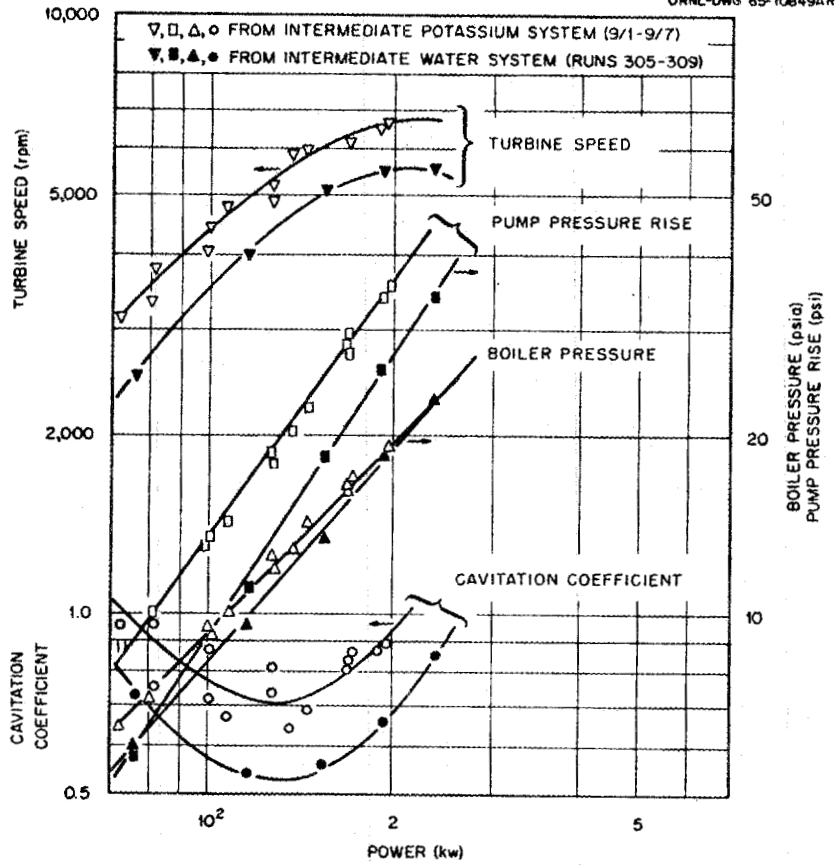


Fig. 3. Effect of IWS and IPS Power Outputs on Principal System Parameters.

ORNL DWG. 64-3546

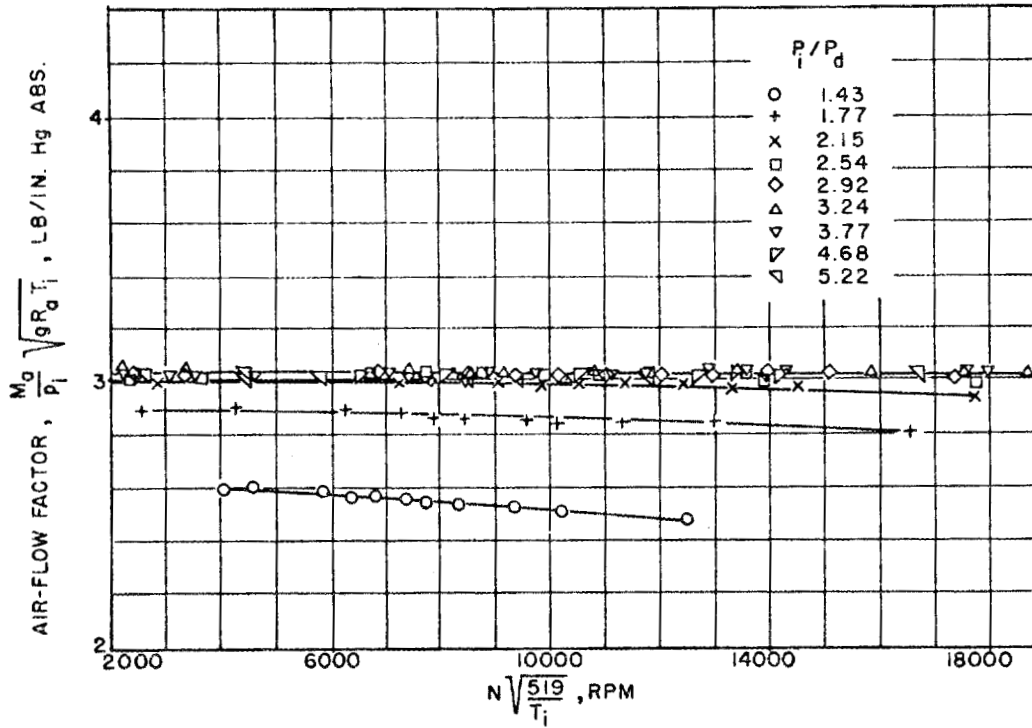


Fig. 4. Effects of Turbine Speed on the Gas Flow Rate with a Constant Pressure Ratio Across a Typical Turbine (Redrawn from Figure 6 of NACA ARC No. E5C30).

probably never be sufficient to produce superheating in the vapor mixture at the condenser inlet. Even if it did, the effect on the radiator performance would be small since the overall cycle efficiency will be only about 15%, so that the increase in the amount of heat to be dumped to space could never exceed 15% of the reactor thermal output. Rough estimates indicate that the increase in mean effective radiator temperature that would stem from the admission of superheated vapor would be sufficient to take care of the extra amount of heat that would have to be dissipated. Thus, so far as the potassium system is concerned, changes in turbine-generator speed and load will have virtually no effect on pressures and flow rates except insofar as the automatic control equipment is designed to respond to changes in the generator output frequency or voltage and actuate the control plugs to change the thermal power output of the reactor.

The system liquid inventory distribution is inherently stable when the components are properly matched. At an appropriate boiler power level, the turbine speed can be adjusted so that the pump discharge pressure will tend to exceed the pressure required to return condensate through the boiler recirculation jet pump and into the boiler. Under this condition, the pump will scavenge liquid from the condenser until there are so many bubbles in the condensate line leaving the condenser that the line pressure drop will increase. With this change, the cavitation suppression head obtained by subcooling will not be sufficient to suppress cavitation in the radiator scavenging jet pump. This unit will cavitate, and its discharge head will drop. This, in turn, will cause the centrifugal feed pump to cavitate, thus decreasing its discharge head and flow. A stable dynamic equilibrium is quickly reached with the pump output reduced sufficiently by cavitation so that the discharge flow rate just matches the system requirements. Operation under this condition is characterized by small rapid fluctuations in the pump discharge pressure (several cycles per second) with the average pump pressure rise less than that which would be produced at this pump speed were the pump not in cavitation.

While cavitation in the feed pump has been used to control the liquid inventory distribution in stationary steam power plants,

many engineers are not familiar with this approach. Since it is an important element in the MPRE system, it seems desirable to present here a detailed picture to give an insight into the problems involved.

In attempting to establish the condensate flow rate leaving the condenser, the first point to observe is that the condenser temperature, and hence the pressure, will depend on the heat dissipation rate. Since the boiler discharge flow rate is limited by a critical pressure drop orifice, the boiler pressure will also depend on (and be directly proportional to) the power output. It is convenient to express the absolute pressures in the region between the condenser and the boiler in terms of the head,  $H$ , in feet of liquid, using the notation of Fig. 5.

At any given boiler power, the pressure and flow rate of the driving stream supplied to the condenser scavenging jet pump will be essentially constant and closely related to the boiler pressure. The pump can be proportioned so that this driving stream will give it a flow capacity greater than the condensate flow rate from the condenser. Thus the jet pump will operate with sufficient vapor ingestion to induce cavitation and reduce its output to the flow rate available.

An insight into the operating mode can be obtained by examining the relations involved. One of these is the cavitation suppression head,  $H_{sv}$ , at the jet pump inlet. This is given by

$$H_{sv} = H_s + H_{sc} - (H_1 - H_2)$$

where  $H_s$  is the static head associated with the difference in level between the condensate manifold and the jet pump,  $H_{sc}$  is the head available from subcooling, and  $H_1 - H_2$  is the head loss associated with the fluid flow from the condensate manifold to the jet pump inlet. The latter can be expressed as

$$H_1 - H_2 = C_1 \frac{G^2}{\rho}$$

where  $C_1$  is a constant that depends on the line diameter and length,

ORNL - DWG 65-5090

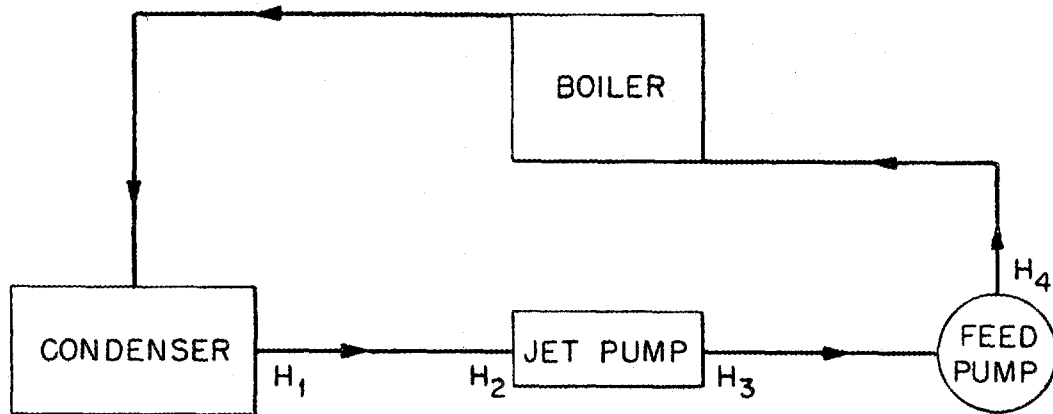


Fig. 5. Liquid System Schematic Diagram Showing the Nomenclature Used to Indicate the Pressures at Key Points in the System.

$G$  is the mass flow rate, and  $\rho$  is the mean density of the bubbly liquid. The static head available from the difference in elevation between the radiator and jet pump deliberately has been made small in the various test rigs being used to simulate the MPRE in order to approximate zero-g conditions; it will, therefore, be neglected here.

It is helpful to consider, in a qualitative fashion, the effects of an increase in the flow rate between the condenser and the jet pump at a constant boiler power output by examining a series of curves. As indicated in Fig. 6, the average fluid density in the line from the condenser to the jet pump will decrease with an increase in mass flow rate, since the liquid flow rate available will remain substantially constant and the concentration of vapor bubbles in the condensate manifold and outlet line will increase. This decrease in density will increase the head loss term,  $H_1 - H_2$ . As the mass flow is increased and the fluid density falls off, condensation in the line of the increasing amount of vapor present will reduce the amount of subcooling that will occur ahead of the jet pump (see Figs. 6 and 7). As the density is reduced, both the increased pressure drop and the reduced amount of subcooling will act to reduce the cavitation suppression head at the jet pump inlet (see Fig. 8). This will reduce the jet pump pressure rise as shown in Fig. 9.

Introducing the effects of cavitation in the feed pump makes the situation somewhat more complex. Basically, the jet pump should be designed so that it has a somewhat greater capacity than the feed pump so that cavitation will begin first in the jet pump. When the delivery head of the jet pump falls off sufficiently, cavitation will begin in the feed pump. The characteristics of the latter are essentially similar to those shown in Fig. 9 for the jet pump, and hence the effects of cavitation in the two pumps are similar to those outlined above for the jet pump alone.

It can be seen from an examination of Figs. 6 to 9 that, with excess capacity in the jet pump and centrifugal feed pump, the liquid inventory distribution should be stable with no liquid in the radiator tubes except the films on the walls because the cavitation suppression head available and the jet pump flow rate increase rapidly with an increase

ORNL-DWG 65-5091

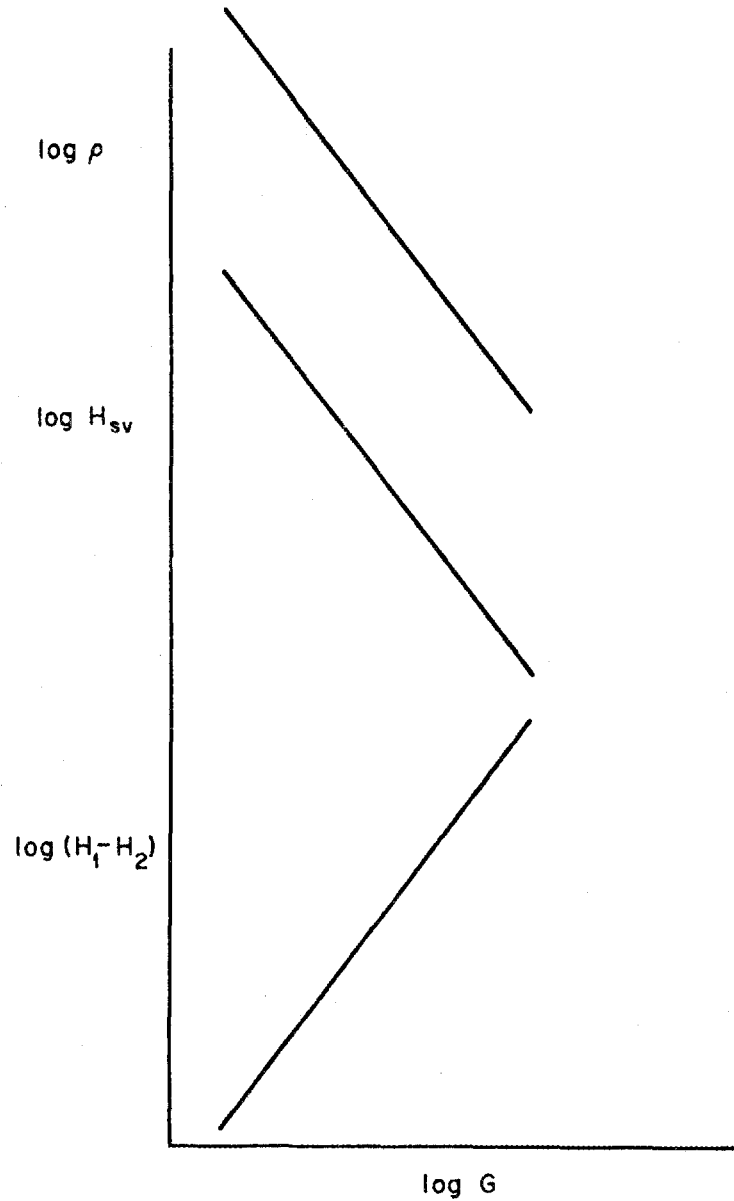


Fig. 6. Average Fluid Density,  $\rho$ , in the Line from the Condenser to the Jet Pump; the Cavitation Suppression Head,  $H_{sv}$ , at the Jet Pump; and the Pressure Drop,  $H_1 - H_2$ , in the Line from the Condenser to the Jet Pump Plotted as Functions of the Mass Flow Rate,  $G$ , Out of the Condenser.

ORNL-DWG 65-5092R

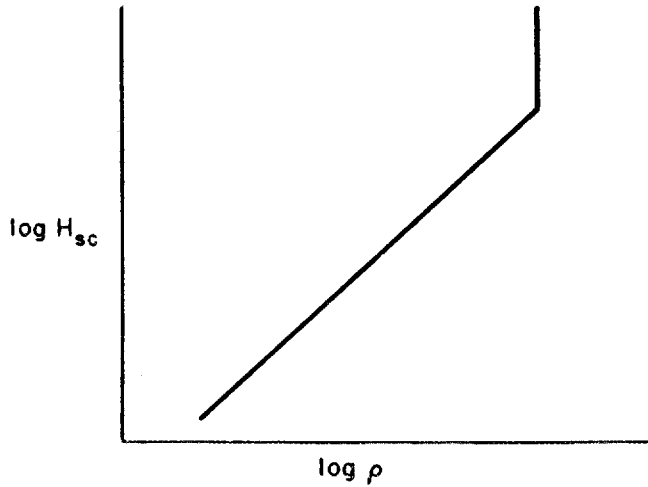


Fig. 7. Relation Between the Contribution to the Cavitation Suppression Head,  $H_{sc}$ , Available from Subcooling and the Average Fluid Density,  $\rho$ , for Flow of Condensate from the Radiator to the Jet Pump.

ORNL-DWG 65-5093R

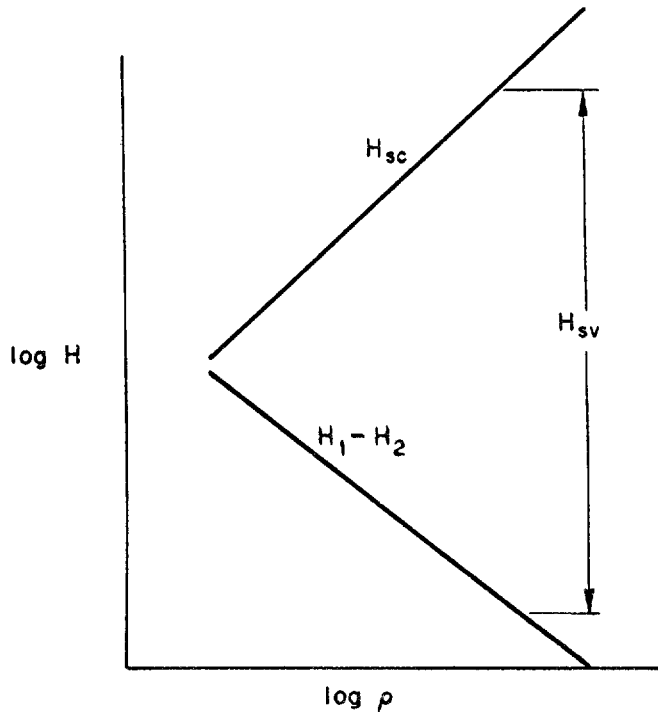


Fig. 8. Relation between the Pressure Drop,  $H_1 - H_2$ , the Contribution to the Cavitation Suppression Head from Subcooling,  $H_{sc}$ , the Cavitation Suppression Head,  $H_{sy}$ , and the Density of the Fluid,  $\rho$ , in the Line between the Condenser and the Jet Pump.

ORNL-DWG 65-5094

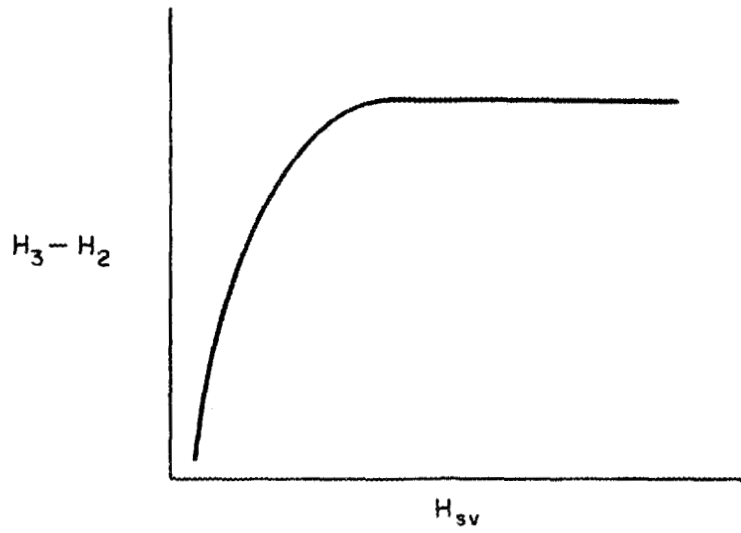


Fig. 9. Typical Curve Showing Effect of Cavitation Suppression Head,  $H_{sv}$ , on Pressure Rise Across a Pump,  $H_1 - H_2$ .

in the liquid density in the condensate line. The jet pump will run cavitating all the time with some vapor bubbles continually entering the condensate outlet manifold of the radiator. Transparent parts in the water systems and infrared photos in the intermediate potassium system<sup>8</sup> clearly show that this operating condition does, in fact, obtain in an actual system. In the range of proportions of interest for both the test rigs and the MPRE, this approach to the control of the liquid inventory distribution is reasonably insensitive to the proportions of the system. Thus, not only will this means of inventory distribution function well over a wide range of power outputs, but it will do so for a fairly wide range of system proportions. An indication of this is that, while two water and three potassium systems have been built and operated in this fashion, only one change has been made in the proportions of the radiator outlet-jet pump region and that was just a change in the diameter of the driving jet in the jet pump of the Intermediate Water System (9l-rod water boiler).

#### PROBLEM AREAS

The stability and control problems of the MPRE system can be clarified somewhat by dividing them into four major items, i.e., the nuclear stability of a boiling potassium fast reactor, stability of the two-phase flows that prevail in the parallel passages of the boiler and condenser, stability of the system as a whole including interactions between components, and stability of the liquid inventory distribution in the system. Each of these problem areas is discussed below.

##### Stability of the Reactor

Thinking about boiling reactors tends to be conditioned by experience with boiling water reactors. Closer inspection indicates that boiling potassium reactors pose a less difficult set of nuclear problems, because the atomic weight of potassium is too high

for it to be a good moderator. Replacing liquid with vapor in the coolant passages of a boiling potassium reactor has little effect on the reactivity, whereas the effects are likely to be very large for water. The reactor can be proportioned in such a way that the difference in reactivity between a core filled with liquid potassium and an empty core is less than one dollar. Thus, cessation of boiling could not induce a violent nuclear excursion, especially since the change in the liquid volume fraction in the coolant passages would rarely exceed 10% during operation.

Reactor proportions giving a negative void coefficient also give negative temperature and power coefficients as a consequence of fuel expansion. Thus, the reactor is inherently stable against either small or large perturbations in temperature, power, or void fraction. These problems as well as other work on the reactor physics are summarized in Ref. 6.

#### Boiling and Condensing Flow Stability

It was recognized at the outset that flow stability in the parallel passages of the boiler had to be assured, and that this presented a major feasibility problem. The problem was attacked experimentally and analytically. Tests with water and Freon<sup>9</sup> turned out quite favorably,<sup>3,4</sup> but great difficulty was experienced with explosive boiling in the early phases of the work with potassium.<sup>7</sup> The inclusion of special nucleation sites near the boiler inlet was found necessary in order both to facilitate starting up the boiler and to maintain stable boiling for normal operation. These nucleation sites have operated for as much as 8000 hr in potassium with no apparent loss in effectiveness.

Analyses indicate that the flow distribution is good,<sup>10</sup> and operation should be stable if the boiler is properly designed and the amount of subcooling at the boiler inlet is small.<sup>11</sup> This holds true even with substantial variations in the radial power distribution. These conclusions are supported by experience with once-through boilers, where intermediate headers have been found to improve the

flow distribution and enhance stability. The interconnecting flow passages of the MPRE constitute, in effect, continuous headers.

While burnout heat flux limitations are important, both analyses and test data indicate that a substantial margin can be provided between normal operating conditions and those that would produce burnout without increasing the reactor size.<sup>12</sup>

Stability of the two-phase flow in the parallel passages of the condenser was also considered to be a potential problem. However, analytical work indicated that condensing flow in the tapered tubes planned for the MPRE system should be stable,<sup>13</sup> and tests with seven different tapered tube condensers have shown excellent flow distribution and flow stability characteristics with only two exceptions; in one instance a poorly proportioned manifold gave a poor distribution under off-design conditions, and large amounts of noncondensables gave poor flow distributions in the condensers of the water systems.<sup>8</sup>

#### Stability of the Complete System

When all of the components of a system are coupled together, it is important that the system as a whole respond well to changes in power. All of the analytical, analog, and electrical test rig experience indicates that the MPRE system is stable and responds well to changes in heat input to the boiler. The mode of operation was described in a previous section. The principal limitations observed are that the thermal inertia of the system is such that it is not possible to increase the "steaming rate" more rapidly than about 1% of full power per second. A reduction in steaming rate ought not exceed about 0.3% per second for a power level change equal to about 20% of full power if foaming in the boiler and the expansion tank are to be avoided. While no difficulty with burnout has been experienced when foaming has been encountered, it appears best to avoid this condition. From the nuclear reactor control standpoint, there is a strong incentive to limit the rate of change of the boiler heat output to about 0.3% per second. A survey of space vehicle

requirements indicates that this is an acceptable value.<sup>14</sup>

### Inventory Distribution

The vapor passages constitute the bulk of the volume in a Rankine cycle fluid system. Since it is important that the boiler not run dry, the bulk of the liquid must be kept in that portion of the system in which it belongs and not be allowed to accumulate in some portion of the vapor region. This is accomplished in the MPRE system by keeping the vapor velocities sufficiently high to sweep along any small accumulations of liquid that may form. This can be done throughout the vapor system except close to the outlet of the condenser tubes. The vapor velocity will vary roughly as the square root of the absolute temperature. This leads to only a 12% decrease in velocity in the vapor region at boiler pressure in going from full to 10% power. In the condenser outlet region the effect is much greater, but there the passage diameters have been made sufficiently small that surface tension will draw the thick liquid film on the walls into slugs of liquid interspersed between bubbles. Thus the problem of maintaining the desired liquid inventory distribution becomes one of assuring that the condenser will be scavenged at all times so that it will be maintained in a "dry sump" condition. A portion of the work with the analog and the electrically heated system mockups has been concerned with this problem. Work with both the analog and the test rigs has shown that, by operating with the boiler feed pump cavitating, the liquid inventory distribution is stable and no control action need be exercised by the operator to allow for changes in power, condenser temperature, or the like.

### MPRE FLUID SYSTEM ANALYSIS

Preliminary analyses of the problem of system flow distribution, stability, and control have been presented in previous reports.<sup>1,15,16</sup> From this work a calculational procedure has evolved that gives a comprehensive analytical tool for investigating the effects of any

system parameter on the flow and pressure distribution. The present work is concerned with the latter problem in the steady-state. This analysis does not purport to treat the stability or control of the system, except insofar as they are involved in the transition from one steady-state to another. Specifically, because of the use of steady-state equations throughout, treatment of dynamic stability is excluded, although sensitivity coefficients for any parameter are readily determined.

A simplified diagram of the system used as the model for this analysis is shown in Fig. 10. The governing equations for the static behavior of this system were derived and means devised for their solution. Because of the implicit nature of many of the relationships, an iterative solution of the system equations is required for the most part. The digital-computer program written for this purpose is an off-design-point program with which system operating conditions may be determined, given a set of system parameters.

A first step in the analysis was to set up the equations interrelating system parameters with component characteristics and operating conditions. The set of equations used in this analysis is presented in Appendix A in approximately the order of solution used by the program. The equations include empirical expressions designed to fit the experimentally determined component characteristics. Comparisons between experimental data<sup>17-22</sup> and empirically derived relations are shown in Figs. 11 through 18.

For the free-turbine-pump unit, Figs. 11 through 13 show the pump head coefficient, the unit overall efficiency, and the ratio of bearing-lubricant flow to total pump flow, respectively, all as functions of the flow coefficient.<sup>17</sup> The equations derived to represent the data are (A-47), (A-48), and (A-49), respectively.

The pressure-ratio and flow-ratio intercepts, respectively, for the jet-pump-flow characteristics are shown as functions of the nozzle-to-throat area ratio in Figs. 14 and 15. The corresponding equations<sup>18</sup> are (A-17) and (A-18), in that order, (A-18) being the same as that used by Cunningham<sup>18</sup> except for a reordering for computational convenience.

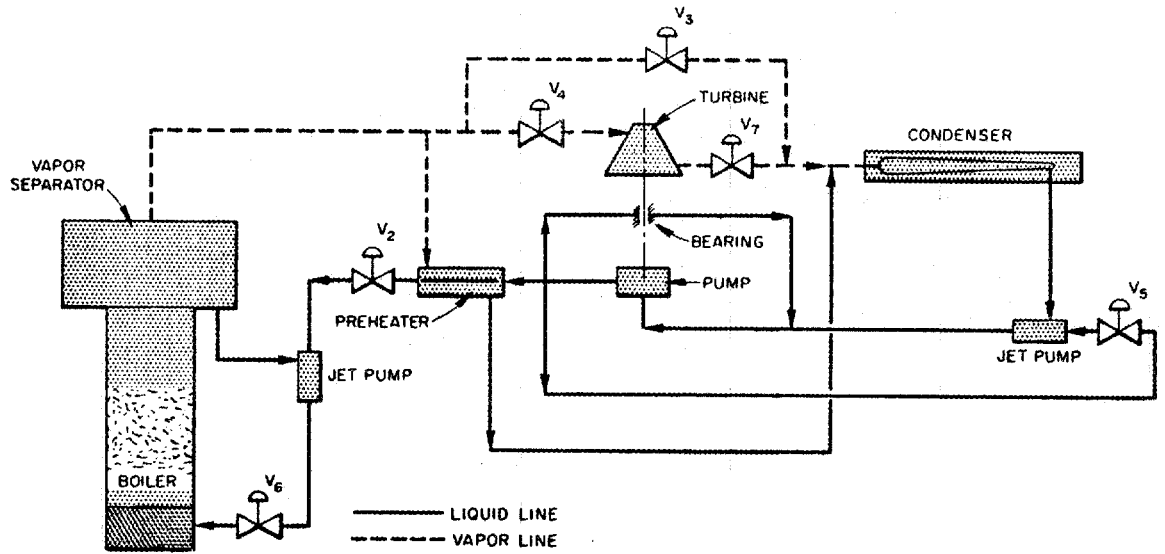


Fig. 10. Simplified Flow Diagram of Boiler System.

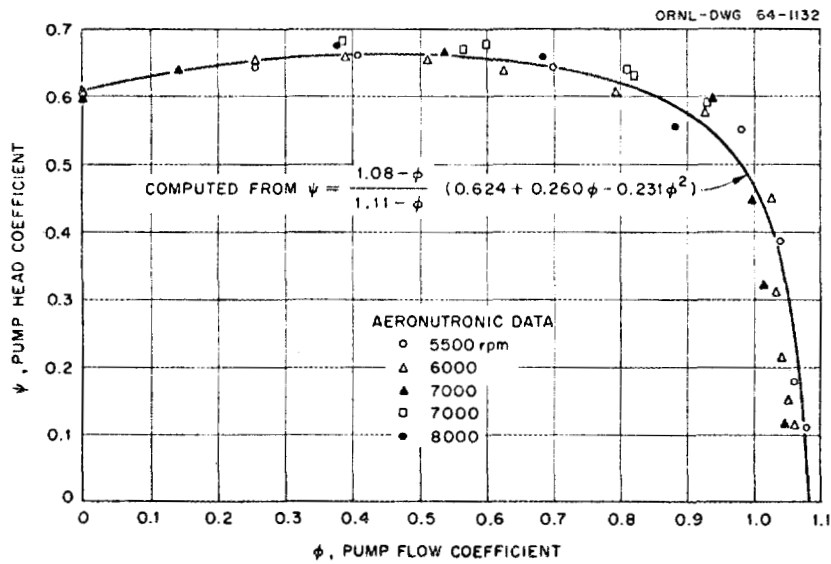


Fig. 11. Pump Head Coefficient as a Function of Pump Flow Coefficient. Comparison of test data with the empirical expression for centrifugal feed-pump performance. Ford Aeronutronic turbine-driven pump, Model S-1.

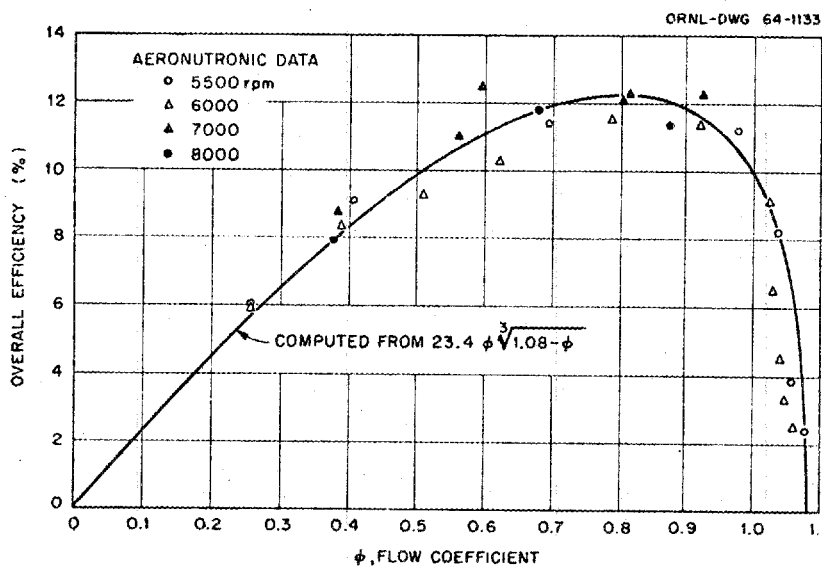


Fig. 12. Overall Turbine-Pump Efficiency as a Function of Pump Flow Coefficient. Comparison of test data with the empirical expression for overall efficiency for the free-turbine-pump unit. Ford Aeronutronic turbine-driven pump, Model S-1.

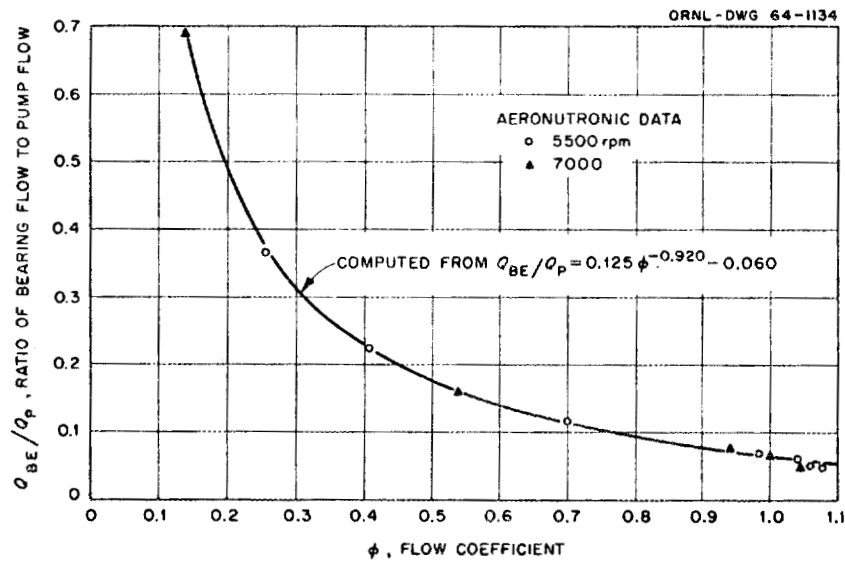


Fig. 13. Ratio of Bearing Lubricant Flow to Pump Flow as a Function of Pump Flow Coefficient. Comparison of test data with the empirical expression for the bearing lubricant flow in the free-turbine-pump unit. Ford Aeronutronic turbine-driven pump, Model S-1.

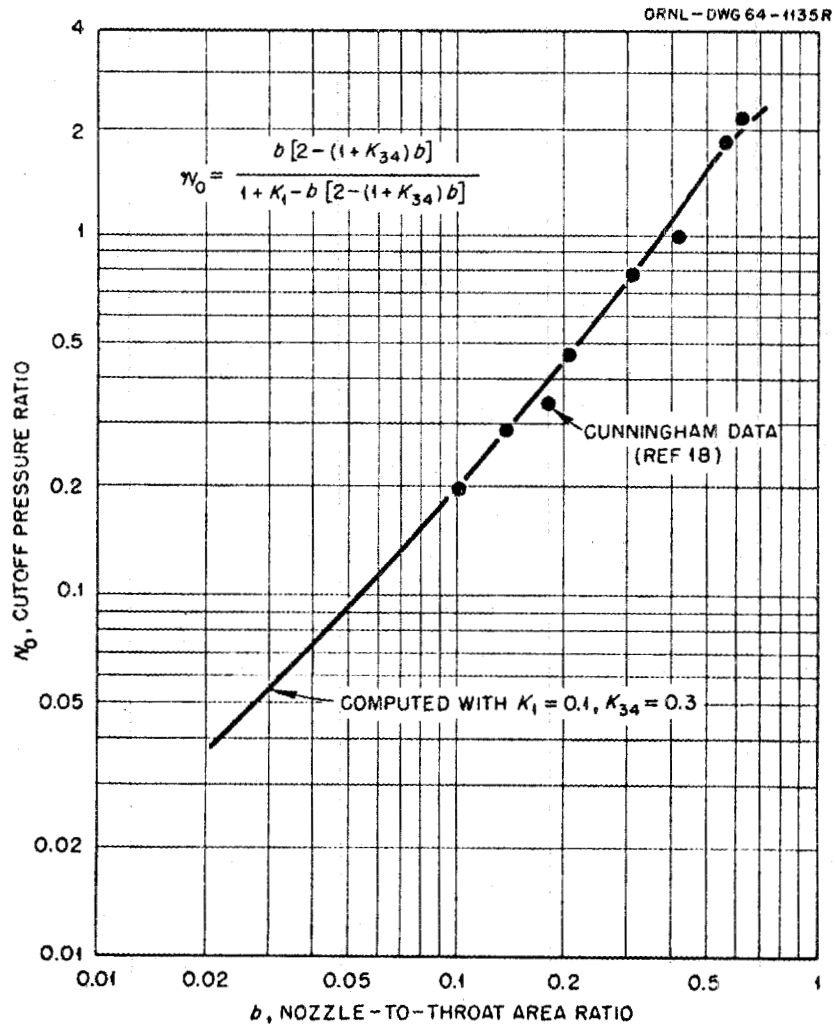


Fig. 14. Jet-Pump Pressure Ratio at Flow Cutoff as a Function of Nozzle-to-Throat Area Ratio. Comparison of test data with semiempirical expression for pressure ratio.

ORNL-DWG 64-1136R

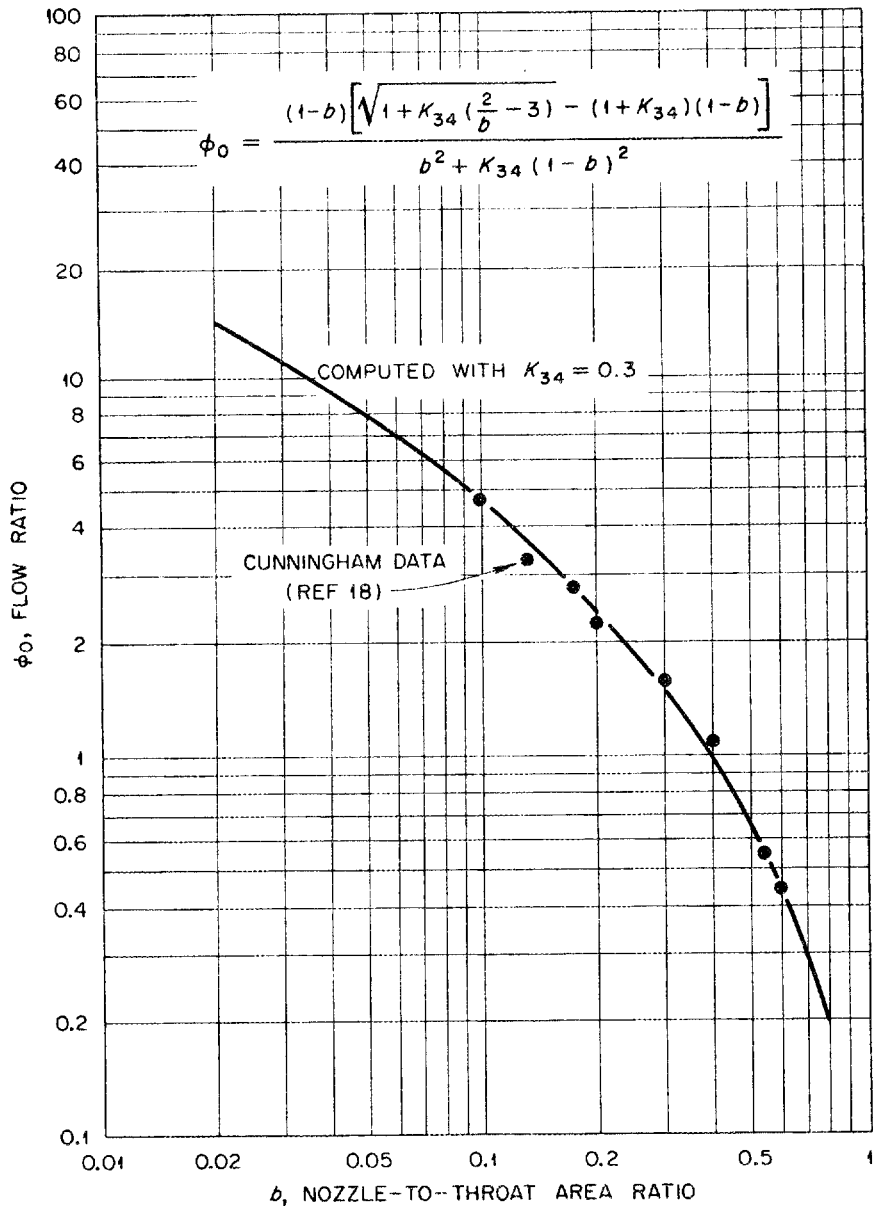


Fig. 15. Jet-Pump Flow Ratio at Zero Pressure Rise as a Function of Nozzle-to-Throat Area Ratio. Comparison of test data with empirical expression for flow ratio.

Figure 16 presents a comparison between experimental void fractions<sup>19</sup> and those determined from equation (B-3) on the basis of constant slip ratio. It can be seen that a narrow range of slips is sufficient to bracket the data, with the mean value of five defining a curve through the data about as well as any. The assumption that the slip is dependent on pressure and, hence, the fluid properties but is independent of quality is basic to the development of the two-phase pressure drop equations of Appendix B.

The empirical relations used to calculate the two-phase pressure drop in the boiler are presented in Appendix B. Figure 17 shows a comparison of the calculated with measured pressure drops,<sup>20</sup> using the slip-ratio relation of Appendix B.

In order to account for superheating of the vapor flowing to the turbine-pump as a consequence of throttling by the upstream valve, approximate values of the Joule-Thomson coefficient were found from vapor tables for both potassium<sup>21</sup> and light water.<sup>22</sup> An isenthalpic expansion from saturation conditions was assumed and the corresponding temperature change determined by tabular interpolation. The resulting coefficients are shown in Fig. 18 together with the empirical expressions derived for computer representation.

#### Results of Computer Calculations

Results from computer runs are presented in Figs. 19 through 24 as examples of the type of information available from the calculations.

Figures 19 through 22 are from runs designed to investigate the effects of variations in jet-pump proportions. Results are for potassium at the design conditions of 1540°F and 364 kw of the Intermediate Potassium System test rig.<sup>4</sup>

The mismatch between the pump pressure rise available and that required is presented in Fig. 19 as a function of the condenser jet-pump flow ratio for several area ratios and nozzle diameters. For each area ratio and nozzle diameter, several values of the bypass valve setting were selected and the system equations iterated to yield values for the mismatch. The curves of Fig. 19 clearly show that

ORNL DWG. 66-2069

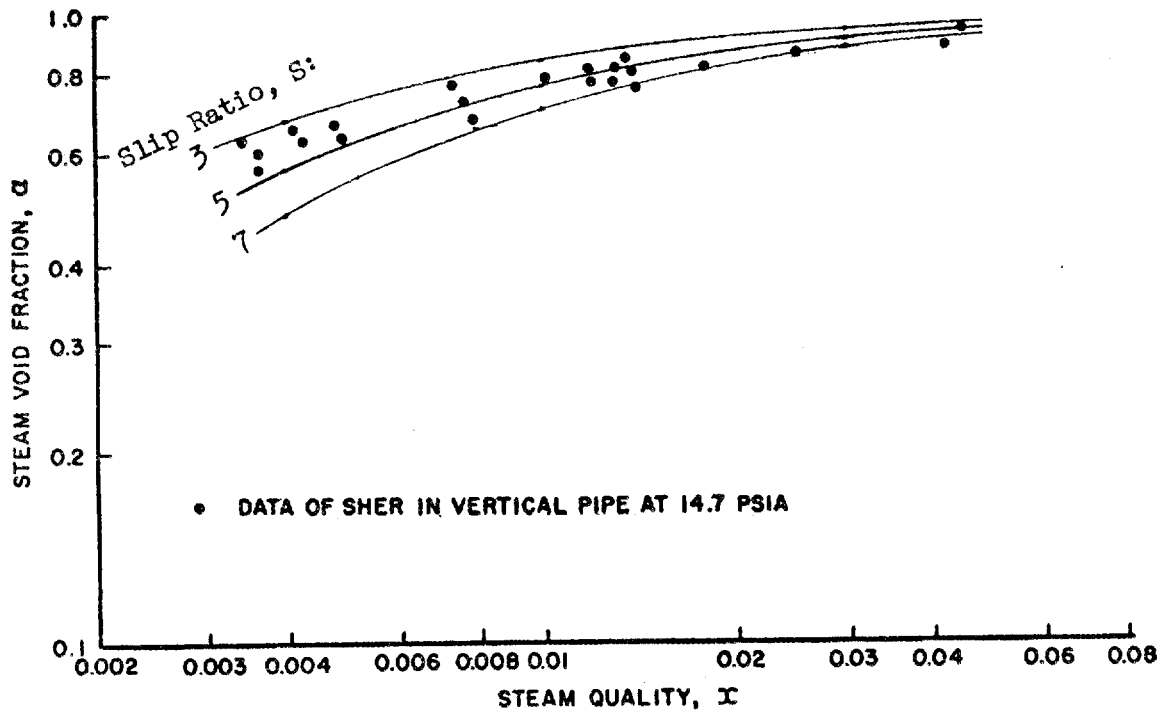


Fig. 16. Comparison of Experimental Void Fractions with Those Computed on the Basis of Constant Slip Ratio.

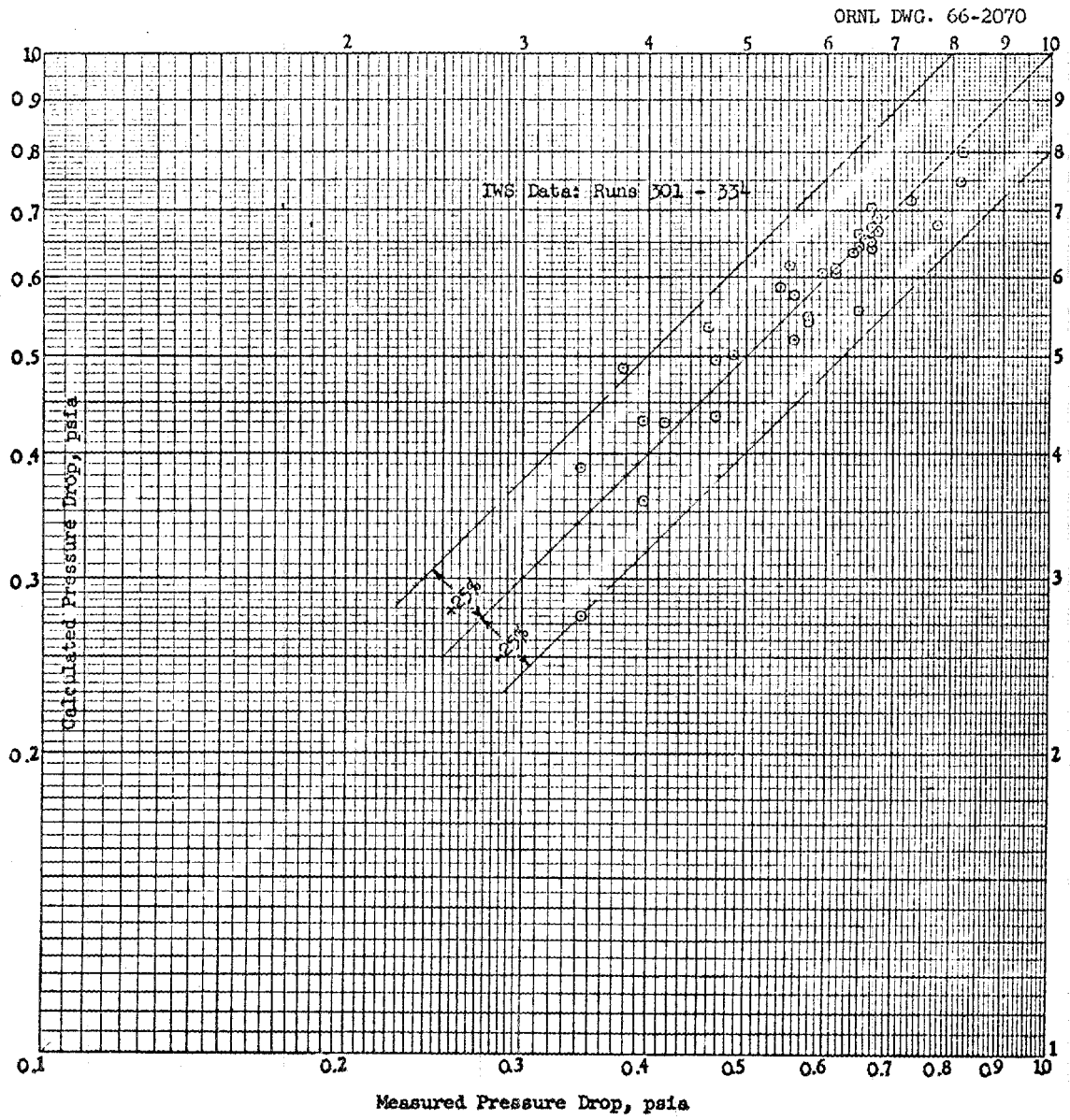


Fig. 17. Comparison Between Measured and Calculated Pressure Drops.  
 Calculated slip ratio =  $0.16 \sqrt[3]{v_g/v_f}$ .

ORNL DWG. 66-2071

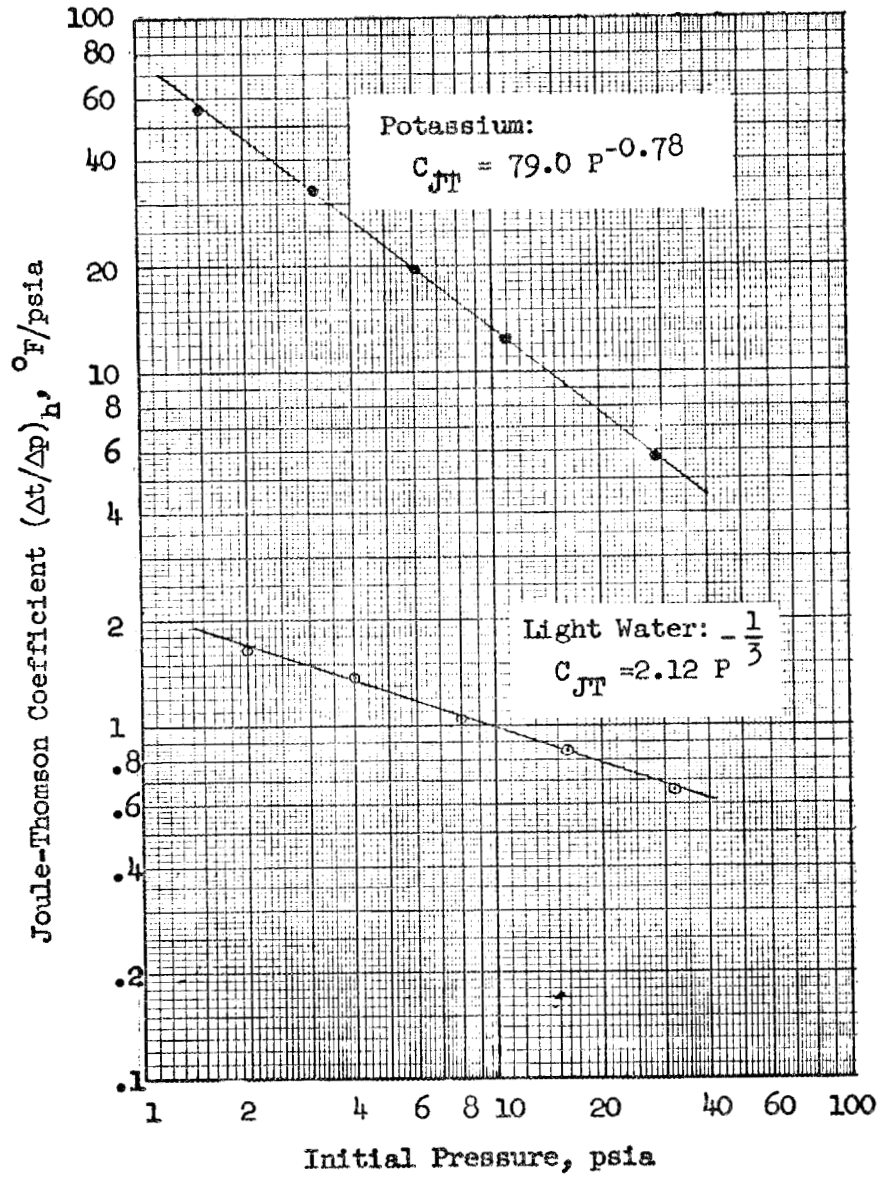


Fig. 18. Approximate Joule-Thomson Coefficients for Potassium and Steam.

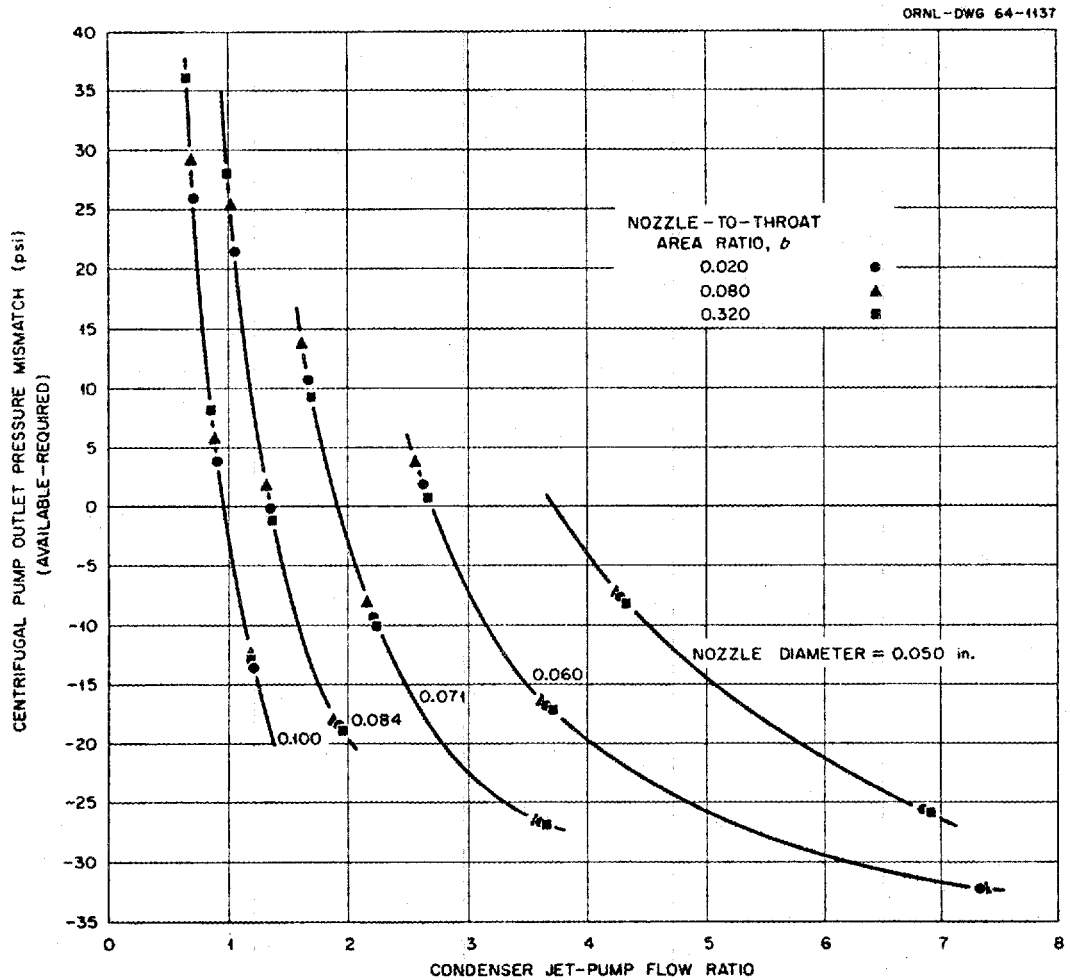


Fig. 19. Centrifugal Pump Pressure Mismatch as a Function of Condenser Jet Pump Flow Ratio for Several Jet Nozzle Diameters and Nozzle-to-Throat Area Ratios.

the mismatch is not dependent on area ratio but is dependent only on nozzle diameter.

A cross-plot of Fig. 19 at zero mismatch then yields Fig. 20, which shows the effect of nozzle diameter on condenser jet-pump flow ratio at design conditions for a balanced system.

Figures 21 and 22 show the effects of boiler jet-pump proportions on the boiler operating quality. It is to be noted that, in Fig. 21, the curves for all nozzle diameters converge on a limiting quality of 29.8%, both as the area ratio,  $b$ ., approaches zero and as it approaches a value of approximately 0.2. For all values of  $b$  greater than 0.2, the quality remains constant at 29.8%. That this shape of the curves is plausible can be seen from the following physical argument. For  $b$ 's approaching zero (corresponding to very large throats), the efficiency of energy transfer and, as a consequence, the pressure rise in the pumped fluid approach zero. With zero pressure rise in the jet-pump, the boiler then functions at a quality characteristic of its operation as a natural circulation system, in this case giving a vapor exit quality of 29.8%, independent of jet-pump proportions. The line marked "cutoff quality" defines the quality, for any value of  $b$ , for zero pressure rise in the jet pump. This "cutoff" line yields a quality of 29.8% for  $b = 0.2$ , thus defining the right-hand convergence point for all of the constant-nozzle-diameter curves.

A constant-quality cross-plot derivable from curves such as those of Fig. 21 is shown in the form of the solid line curves in Fig. 22. The dashed line curves represent the relation between nozzle diameter and  $b$  at a constant throat diameter as derived from the definition of  $b$ . The intersections of the two sets of lines then show the operating qualities and the corresponding jet-pump proportions.

As indicated previously, a cardinal principle in the system operation is the use of critical flow through key restrictions in the vapor lines in order to yield a unique relation between power and the boiler pressure and vapor production. Figure 23 was prepared from a series of computer runs as an aid in the selection of the appropriate values for the resistances, upstream and downstream of the turbine, required for any desired operating condition. Line ABCD delineates

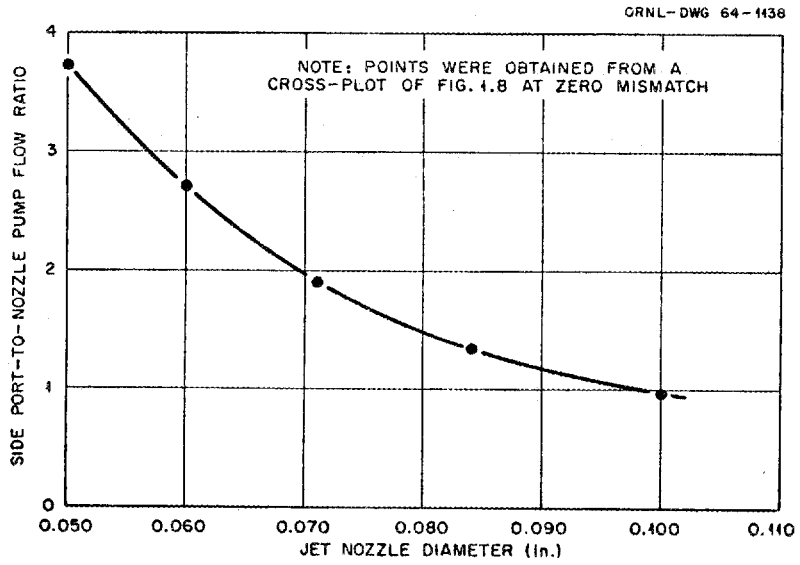


Fig. 20. Condenser Jet-Pump Flow Ratio at Design Conditions as a Function of Jet Nozzle Diameter.

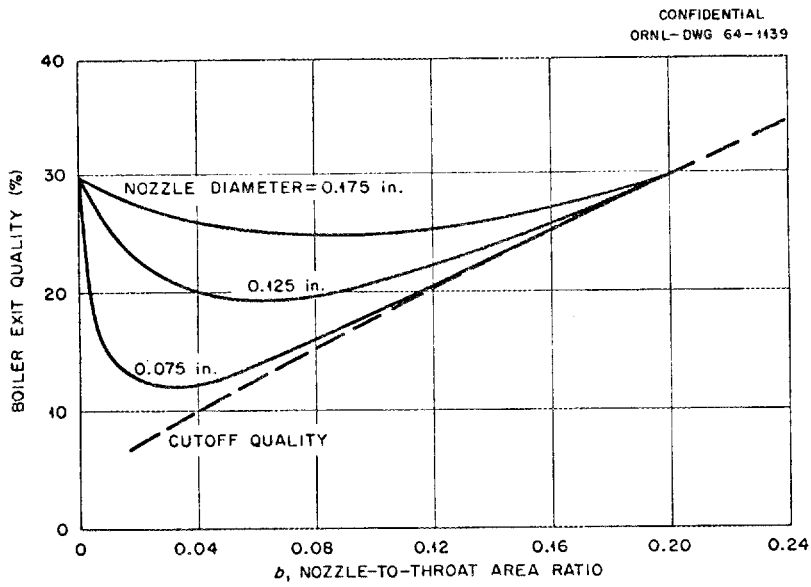


Fig. 21. Boiler Exit Quality as a Function of Nozzle-to-Throat Area Ratio at Constant Jet-Pump Nozzle Diameter.

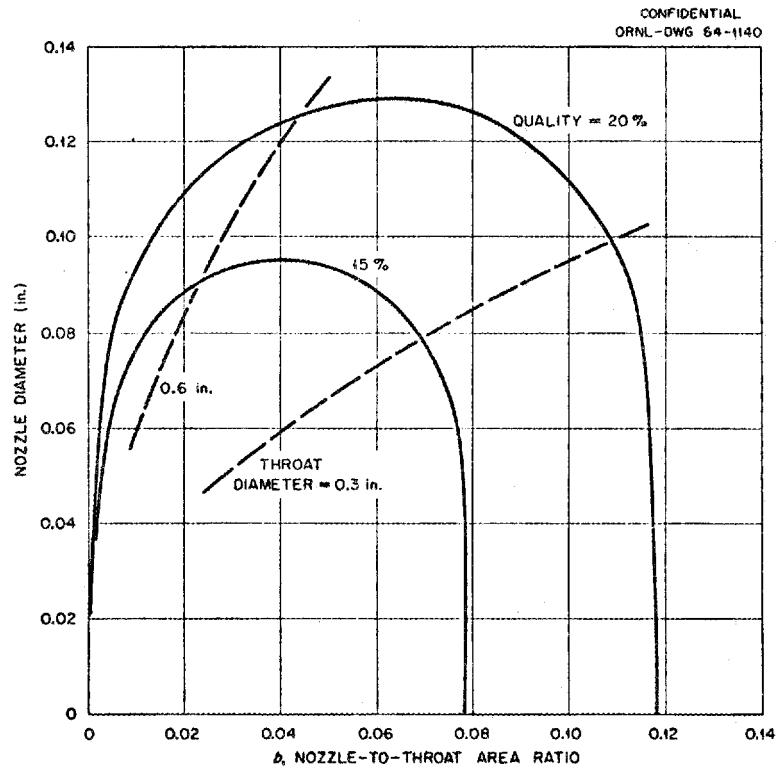


Fig. 22. Boiler Jet-Pump Nozzle Diameter as a Function of Nozzle-to-Throat Area Ratio at Constant Quality and at Constant Throat Diameter.

ORNL DWG. 66-2072

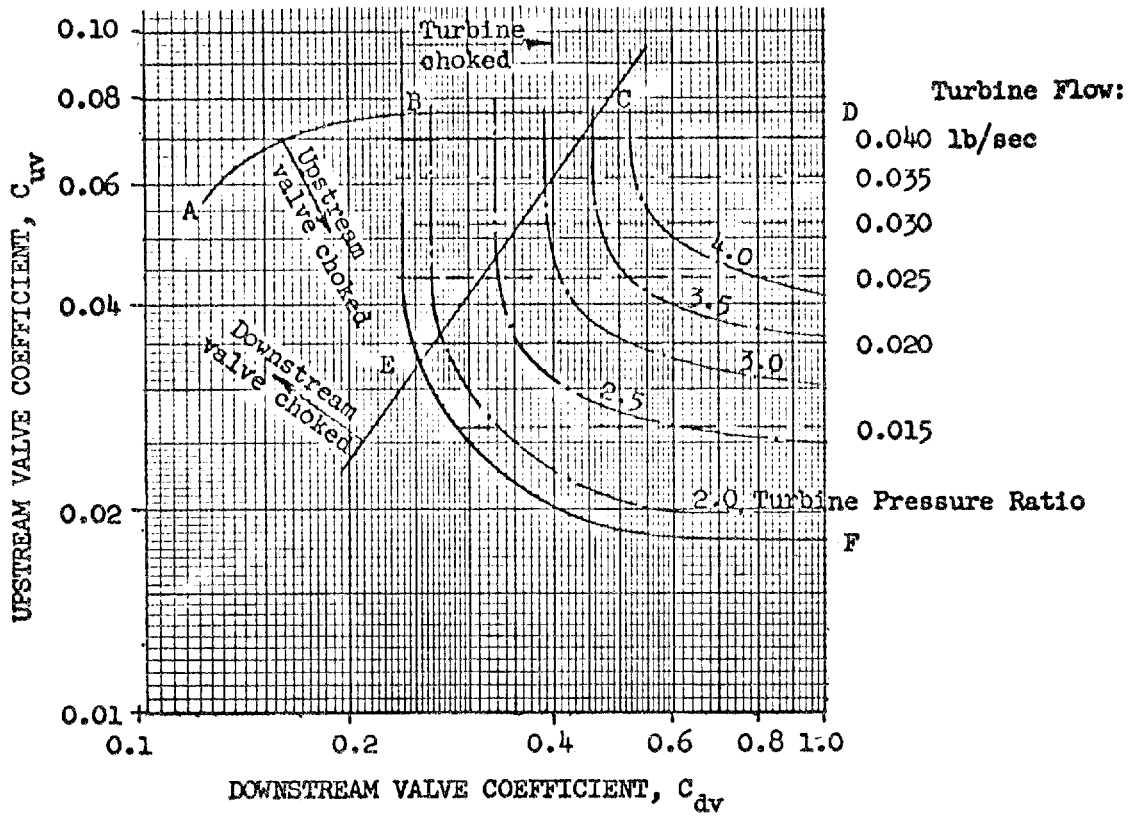


Fig. 23. Operating Map for Free-Turbine-Pump Unit in Intermediate Water System at 14.7 psia Boiler Pressure.

the boundary below which the upstream valve is choked. Similarly, line BEF establishes the region in which the turbine operates with choked nozzles, i.e., to the right and above BEF. Finally, the downstream valve is found to be choked above and to the left of line CE. Lines of constant turbine flow and turbine pressure ratio have been superimposed on the region defined by DBEF, i.e., the region in which both the turbine and the upstream valve are choked. Operation of both the actual system and its analog is normally restricted to region DCEF, where the downstream valve is not choked.

A comparison is made in Fig. 24 between IWS data and its calculated counterpart. The IWS data was matched in the vicinity of 3.0 kw per rod; a series of computer runs was then made with varying boiler power and the results compared as shown in the figure. As can be seen, the agreement between experimental and calculated values of pump pressure rise and boiler pressure is excellent. The comparison does not fare nearly so well, however, in the case of pump speed. Possibly the discrepancy stems from a difference between the turbine-pump overall efficiency determined from bench tests and that obtaining with the unit installed in the test loop. The computer program currently uses the original bench test data for efficiency, whereas the pump in the test rig has been reworked to reduce the load on the thrust bearing.

#### CONCLUSIONS

Detailed digital computer calculations have shown that the basic control concepts for system operation as set forth in the first portion of this report are sound, and that the system can be proportioned and the various components matched so that the only control action required over a wide range of powers is control of the heat input to the boiler. Experience with system mockups operating both with water and with potassium has shown that the systems operate essentially as predicted by digital computer calculations. For example, the computer results

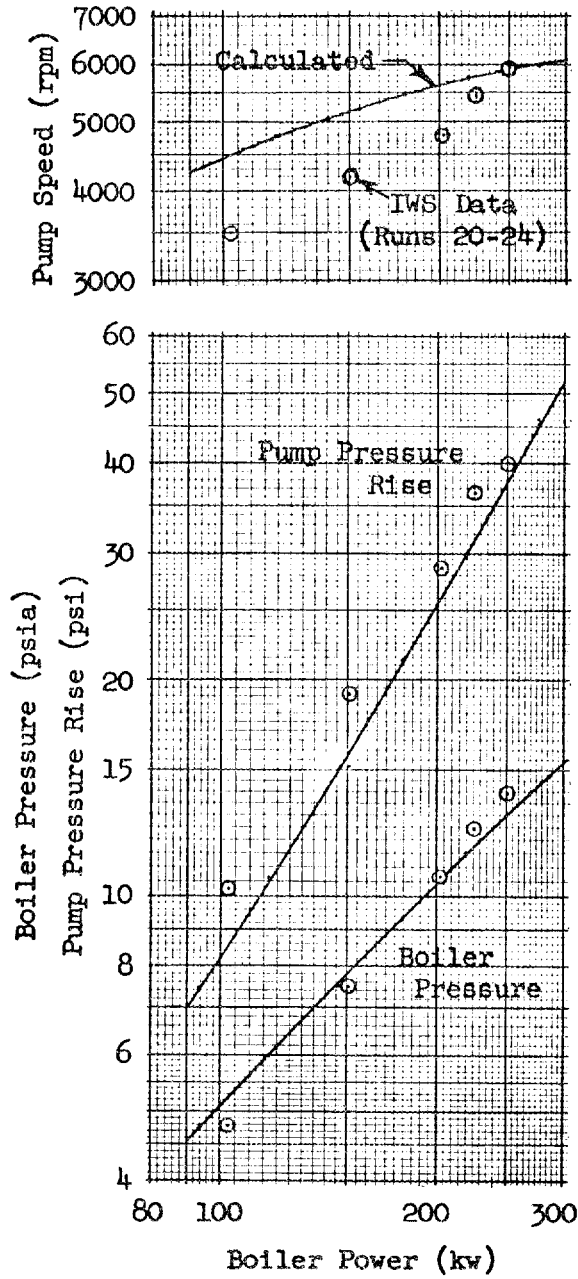


Fig. 24. Comparison between Calculated and Experimental Parameters for Intermediate Water System.

show that, over a wide operating range, the output of the free-turbine-driven centrifugal feed pump exceeds that required, thus ensuring control of the liquid inventory distribution through cavitation in the feed pump. The experimental systems tested yield the same conclusion.

A detailed analysis of the flow and pressure distribution throughout the MPRE system has been carried out with experimental component characteristics utilized wherever available. The resulting digital computer program has provided a ready means for evaluating the effects of changes in component characteristics and operating conditions. The utility of any proposed system modification can be evaluated quickly and at minimum expense with a digital computer calculation.

The digital computer code has been useful in the proportioning of experimental systems in order to achieve the desired operating characteristics. The jet pump proportions for the IPS were so determined; the system has operated quite satisfactorily with these pumps.

An essential part of the overall computational scheme is the ability to determine pressure drop during boiling. The two-phase pressure drop equations developed in this report, while perhaps ad hoc, provide a reliable means for predicting reactor core pressure drops.



.



~~CONFIDENTIAL~~

APPENDICES

~~CONFIDENTIAL~~



APPENDIX A

## SYSTEM EQUATIONS

The equations used in this analysis are listed below in approximately the order in which they are encountered during execution of the computer program.

Turbine Equations

Critical pressure ratio,  $R_{cr}$ :

$$R_{cr} = \left( \frac{K + 1}{2} \right)^{\frac{K}{K - 1}} \quad (A-1)$$

where  $K$  = ratio of vapor specific heats.

Upstream valve critical flow,  $M_{uvc}$  (lb<sub>m</sub>/sec):

$$M_{uvc} = \frac{C_{uv} P_b}{\sqrt{T_b}} \quad , \quad (A-2)$$

where

$C_{uv}$  = upstream valve conductance coefficient,

$P_b$  = boiler exit pressure, psia,

$T_b$  = boiler exit temperature, °R.

Upstream valve pressure ratio,  $R_{uv}$ :

$$R_{uv} = \frac{P_b}{P_t} \quad , \quad (A-3)$$

where

$P_t$  = turbine inlet pressure, psia.

Upstream valve flow,  $M_{uv}$  ( $lb_m/sec$ ):

$$M_{uv} = M_{uvc} F(R_{uv}), \quad (A-4)$$

where

$$F(U) = \left( \frac{K+1}{2} \right)^{\frac{1}{K-1}} \sqrt{\frac{K+1}{K-1}} \left[ U^{\frac{2}{K}} - U^{\frac{K+1}{K}} \right] \text{ for } U < R_{cr} \quad (A-5)$$

$$= 1 \quad \text{for } U \geq R_{cr}$$

Downstream valve critical flow,  $M_{dvc}$  ( $lb_m/sec$ ):

$$M_{dvc} = \frac{C_{dv} P_{dv}}{\sqrt{T_{dv}}}, \quad (A-6)$$

where

$C_{dv}$  = downstream valve conductance coefficient,

$P_{dv}$  = turbine exit pressure, psia,

$T_{dv}$  = vapor temperature corresponding to  $P_{dv}$ , °R.

Downstream valve pressure ratio,  $R_{dv}$ :

$$R_{dv} = \frac{P_{dv}}{P_c}, \quad (A-7)$$

where

$P_c$  = condenser pressure, psia.

Downstream valve flow,  $M_{dv}$  (lb<sub>m</sub>/sec):

$$M_{dv} = M_{dvc} F(R_{dv}) \quad , \quad (A-8)$$

where  $F(R_{dv})$  is as previously defined.

Continuity requirement:

$$M_{dv} = M_{uv} \quad , \quad (A-9)$$

by iteration on  $P_{dv}$ .

Joule-Thomson coefficient,  $C_{JT}$  (°R-in.<sup>2</sup>/lb<sub>f</sub>):

for light water,

$$C_{JT} = 2.12 P^{-\frac{1}{3}} \quad ; \quad (A-10a)$$

for potassium,

$$C_{JT} = 79.0 P^{-0.78} \quad (A-10b)$$

where  $P$  is the initial pressure for an isenthalpic expansion.

Turbine inlet temperature,  $T_t$  (°R):

$$T_t = T_b - C_{JT} (P_b - P_t) \quad , \quad (A-11)$$

Turbine critical flow,  $M_{tc}$  (lb<sub>m</sub>/sec):

$$M_{tc} = \sqrt{\frac{g_c K}{R} \left( \frac{2}{K+1} \right)^{\frac{K+1}{K-1}} \frac{A_t P_t}{\sqrt{T_t}}} \quad (A-12)$$

where

$$g_c = 32.174 \text{ (lb}_m/\text{lb}_f) \text{ (ft/sec}^2) \quad ,$$

$$R = \text{gas constant, ft-lb}_f/\text{lb}_m \text{-}^\circ\text{R} \quad ,$$

$$A_t = \text{turbine-nozzle throat area, in.}^2$$

Turbine pressure ratio,  $R_t$ :

$$R_t = \frac{P_t}{P_{dv}} \quad (A-13)$$

Turbine flow,  $M_t$  (lb<sub>m</sub>/sec):

$$M_t = M_{tc} F(R_t) \quad , \quad (A-14)$$

where  $F(R_t)$  is as previously defined by Eq. (A-5).

Continuity requirement:

$$M_t = M_{uv} \quad , \quad (A-15)$$

by iteration on  $P_t$ .

Bypass valve flow,  $M_v$  (lb<sub>m</sub>/sec):

$$M_v = \frac{C_v P_b}{\sqrt{T_b}} \quad , \quad (A-16)$$

where

$C_v$  = bypass valve conductance coefficient.

#### Jet-Pump Equations

Maximum pressure ratio,  $N_o$  :

$$N_o = \frac{b(2 - 1.3b)}{1.1 - b(2 - 1.3b)} \quad (A-17)$$

where  $b$  = nozzle-to-throat area ratio.

Maximum flow ratio,  $\Phi_o$  :

$$\Phi_o = \frac{(1 - b) \left[ \sqrt{1 + 0.3 \left( \frac{2}{b} - 3 \right)} - 1.3(1 - b) \right]}{b^2 + 0.3(1 - b)^2} \quad (A-18)$$

Pressure ratio, N:

$$N = \frac{N_1}{1.1 - N_1} \quad (A-19)$$

where

$$N_1 = b \left[ 2+b \left\{ (1-2b) \frac{\Phi^2}{(1-b)^2} - 1.3(1+\Phi)^2 \right\} \right] \text{ for } \Phi < \Phi_o$$

$$= 0 \quad \text{for } \Phi > \Phi_o$$

(A-20)

Boiler Equations

Feed-heater flow, hot side,  $M_F$  (lb<sub>m</sub>/sec):

$$M_F = \frac{C_f P_b}{\sqrt{T_b}} \quad (A-21)$$

where

$C_f$  = feed-heater conductance coefficient.

Total vapor flow,  $M_b$  (lb<sub>m</sub>/sec):

$$M_b = M_F + M_t + M_v \quad (A-22)$$

Power required,  $p$  (kw):

$$p = 1.05487 \left[ H_{fg} (M_b - M_f) + C_p M_b (T_b - T_c) \right] , \quad (A-23)$$

where

$H_{fg}$  = latent heat, Btu/lb<sub>m</sub> ,

$C_p$  = liquid specific heat, Btu/lb<sub>m</sub> - °R ,

$T_c$  = condensate temperature, °R .

Total flow into boiler,  $M$  (lb<sub>m</sub>/sec):

$$M = \frac{M_b}{x} , \quad (A-24)$$

where

$x$  = vapor quality.

Feed-heater exit temperature, cold side,  $T_f$  (°R):

$$T_e = T_c + \frac{H_{fg} M_f}{C_p M_b} . \quad (A-25)$$

Boiler inlet temperature,  $T_i$  (°R):

$$T_i = x T_e + (1 - x) T_b . \quad (A-26)$$

Preheater length,  $L_p$  (in.):

$$L_p = 1.05487 C_p (T_b - T_i) M L_h / p , \quad (A-27)$$

where

$L_h$  = heated length in boiler matrix, in.

Boiling length,  $L_b$  (in.):

$$L_b = L_b - L_p \quad . \quad (A-28)$$

Boiler pressure drop,  $\Delta P_b$  (psi):

$$\Delta P_b = \Delta P_f + \Delta P_a + \Delta P_h \quad , \quad (A-29)$$

where

$\Delta P_f$ ,  $\Delta P_a$ , and  $\Delta P_h$  are the friction, acceleration, and static head components of the boiler pressure drop computed as shown in Appendix B.

#### Boiler Jet-Pump Equations

Flow ratio,  $\Phi_b$ :

$$\Phi_b = \frac{1 - x}{x} \quad . \quad (A-30)$$

Pressure ratio,  $N_b$ :

$$N_b = \frac{N_{1b}}{1.1 - N_{1b}} \quad , \quad (A-31)$$

where  $N_{1b}$  is defined by Eq. (A-20).

Side port pressure,  $P_{sb}$  (psia):

$$P_{sb} = P_b + \frac{gZ_b}{1728g_c v_{fb}} \quad , \quad (A-32)$$

where

$g$  = local gravitational acceleration,  $f/sec^2$  ,

$Z_b$  = static head from vapor separator, in. ,

$v_{fb}$  = liquid specific volume, ft<sup>3</sup>/lb.

Nozzle inlet pressure,  $P_{nb}$  (psia):

$$P_{nb} = P_{sb} + \frac{v_{fe} M_b^2}{C_{nb}}, \quad (A-33)$$

where

$C_{nb}$  = boiler jet-pump-nozzle conductance coefficient ,

$v_{fe}$  = liquid specific volume, ft<sup>3</sup>/lb<sub>m</sub> .

Discharge pressure,  $P_{db}$  (psia):

$$P_{db} = \frac{P_{sb} + N_b P_{nb}}{1 + N_b} . \quad (A-34)$$

Available jet-pump pressure rise,  $\Delta P_j$  (psia):

$$\Delta P_j = P_{db} + \frac{gZ_d}{1738g_c v_{fd}} - \frac{v_{fd} M^2}{C_b}, \quad (A-35)$$

where

$Z_d$  = static head, side port to boiler inlet, in. ,

$v_{fd}$  = liquid specific volume, ft<sup>3</sup>/lb<sub>m</sub> ,

$C_b$  = jet-pump-outlet trim valve conductance coefficient.

Balance requirement:

$$\Delta P_b = \Delta P_j , \quad (A-36)$$

by iteration on vapor quality,  $x$ .

Condenser temperature, space radiator ( $^{\circ}\text{R}$ ):

$$T_c = T_{co} \sqrt[4]{\frac{p}{p_o}}, \quad (\text{A-37})$$

where  $T_{co}$  and  $p_o$  are design values.

Condenser temperature, water-cooled ( $^{\circ}\text{R}$ ):

$$T_c = \frac{T_{co} - T_{wo}}{p_o} p + T_w, \quad (\text{A-38})$$

where

$T_w$  = temperature of cooling water,  $^{\circ}\text{R}$ ,

$T_{wo}$  = design temperature,  $^{\circ}\text{R}$ .

Condenser pressure,  $P_c$  (psia):

$$\log_e P_c = A + \frac{B}{T_c - C}, \quad (\text{A-39})$$

where

A, B, and C are constants determined from a vapor-pressure versus temperature curve.

#### Condenser Jet-Pump Equations

Side-port pressure,  $P_{sc}$  (psia):

$$P_{sc} = P_c + \frac{gZ_c}{1728g_c v_{fc}}, \quad (\text{A-40})$$

where

$Z_c$  = static head, condenser to side-port, in.,

$v_{fc}$  = liquid specific volume,  $\text{ft}^3/\text{lb}_m$ .

Nozzle-inlet pressure,  $P_{nc}$  (psia):

$$P_{nc} = \frac{C_{nc} P_{sc} + C_c P_p}{C_{nc} + C_c}, \quad (\text{A-41})$$

where

$C_{nc}$  = condenser jet-pump-nozzle conductance coefficient,

$C_c$  = jet-pump-nozzle trim valve conductance coefficient,

$P_p$  = centrifugal pump outlet pressure (required), psia.

Nozzle flow,  $M_n$  ( $\text{lb}_m/\text{sec}$ ):

$$M_n = \sqrt{\frac{C_{nc} (P_{nc} - P_{sc})}{v_{fc}}}. \quad (\text{A-42})$$

Flow ratio,  $\Phi_c$ :

$$\Phi_c = \frac{M_b}{M_n}. \quad (\text{A-43})$$

Pressure ratio,  $N_c$ :

$$N_c = \frac{N_{1c}}{1.1 - N_{1c}}, \quad (\text{A-44})$$

where  $N_{1c}$  is defined by Eq. (A-20).

Discharge pressure,  $P_{dc}$  (psia):

$$P_{dc} = \frac{P_{sc} + N_c P_n}{1 + N_c} \quad (A-45)$$

Discharge flow,  $Q_{dc}$  (gpm):

$$Q_{dc} = 448.831 v_{fc} (M_b + M_n) \quad (A-46)$$

### Centrifugal Pump Equations

Head coefficient,  $\psi$ :

$$\psi = \frac{1.08 - \Phi}{1.11 - \Phi} (0.624 + 0.260 \Phi - 0.231 \Phi^2) \quad (A-47)$$

where  $\Phi$  is the pump flow coefficient.

Turbine-pump overall efficiency,  $\eta$ :

$$\eta = 0.234 \Phi \sqrt{1.08 - \Phi} \quad (A-48)$$

Bearing flow coefficient,  $\Phi_{be}$ :

$$\Phi_{be} = 0.125 \Phi^{-0.920} - 0.060 \quad (A-49)$$

Flow,  $Q$  (gpm) and available pressure rise,  $\Delta P_a$  (psi):

$$\frac{\Delta P_a}{Q^2} = \frac{1}{g_c} \left( \frac{231}{144 A_p} \right)^2 \frac{\psi}{v_{fc} \Phi^2} \quad (A-50)$$

$$Q \Delta P_a = 3.11688 A_p P_t \eta R_t^{-1/K} \sqrt{2g_c R T_t \left[ \frac{K}{K-1} \left\{ 1 - R_t \frac{1-K}{K} \right\} \right]^3} \quad (A-51)$$

where

$A_p$  = pump diffuser throat area, in.<sup>2</sup>

Bearing flow,  $Q_{be}$  (gpm):

$$Q_{be} = \Phi_{be} Q \quad . \quad (A-52)$$

Pump inlet flow required,  $Q_i$  (gpm):

$$Q_i = Q_{be} + Q_{dc} \quad . \quad (A-53)$$

Balance requirement:

$$Q = Q_i \quad , \quad (A-54)$$

by iteration on  $\Phi$ .

Pump speed,  $N$  (rpm):

$$N = \frac{231}{\pi D_p A_p} \frac{Q}{\Phi} \quad , \quad (A-55)$$

where

$D_p$  = pump impeller tip diameter, in.

Required pump pressure rise,  $\Delta P_r$  (psi):

$$\Delta P_r = P_{nb} + \frac{v_{fe} M_b^2}{C_p} - P_{dc} \quad , \quad (A-56)$$

where

$C_p$  = pump discharge trim valve conductance coefficient.

Cavitation coefficient,  $C_{cav}$ :

$$C_{cav} = \frac{\Delta P_r}{\Delta P_a} \quad (A-57)$$



APPENDIX B

## TWO-PHASE PRESSURE DROP EQUATIONS

Initial versions of the system program used Owens'<sup>23</sup> method for computing pressure drop in the boiler. However, when data<sup>20</sup> from the Intermediate Water System became available, it was found that the pressure drops were being overestimated by a factor of roughly 2 to 3. While part of this discrepancy undoubtedly stems from the fact that Owens' procedure is basically a homogeneous calculation, his success in correlating the Schrock and Grossman<sup>24</sup> data indicates that this is not the whole story. A homogeneous calculation overestimates the two-phase specific volume and, hence, both the acceleration and friction components, while the static head contribution is underestimated. These latter two errors are at least partially compensating, so that agreement (or the lack of it) may well depend on the proportion of acceleration to overall pressure drop. This conclusion is rendered more plausible by the facts that in the Schrock and Grossman data, which correlated well, the acceleration component was a third or less of the total, whereas in the IWS data, which correlated poorly, the acceleration drop constitutes 60 to 70% of the total.

Homogeneous flow is a first order approximation (to the actual flow) in which slip is assumed to be (a) constant and (b) equal to one for all pressures and qualities. If this latter restriction is relaxed to the extent of allowing the slip to be a function of pressure and, hence, of specific volume ratio, an approximation of penultimate simplicity is obtained. This approximation will be used in what follows in order to match the observed IWS pressure drops. Figure 16 shows the justification for this step. The data are those of Sher<sup>19</sup> for steam and water at 14.7 psia in vertical flow with heat addition. The superimposed curves were computed from the relation between void fraction and quality at constant slip ratio given by Eq. (B-3). As can be seen, a rather narrow range of slip suffices to bracket the data. In fact, the curve for a slip ratio of five fits about as well as the data justify.

Preheating Section Pressure Drop

For the frictional component,

$$\Delta P_{fp} = \frac{fG^2 v_f L_p}{288g_c D_e} , \quad (B-1)$$

where

$f$  = single-phase friction factor,

$G$  = mass flow per unit area,  $\text{lb}_m/\text{sec-ft}^2$ ,

$D_e$  = equivalent diameter of flow passage, in.

For the static head component,

$$\Delta P_{hp} = \frac{g}{g_c} \frac{L_p}{1728v_f} . \quad (B-2)$$

The acceleration component resulting from specific volume changes in the preheating section is extremely small and will be neglected.

Boiling Section Pressure Drop

From continuity and the definition of quality, the void fraction,  $\alpha$ , may be expressed as

$$\alpha = \frac{1}{1 + \beta S \frac{1-x}{x}} , \quad (B-3)$$

where

$\beta$  =  $v_f/v_g$  ,

$S$  = slip ratio = vapor velocity/liquid velocity =  $v_g/v_f$ ,

$v_g$  = vapor specific volume,  $\text{ft}^3/\text{lb}_m$ .

Exit quality,  $x_e$ , is found from

$$x_e = \frac{Q/M - C_p (T_p - T_i)}{H_{fg}}, \quad (\text{B-4})$$

where

$$Q = p/1.05487 = \text{Btu/sec.}$$

For a linear variation with heated length, the quality,  $x$ , is given by

$$x = \frac{x_e L}{L_h - L_p}, \quad (\text{B-5})$$

where

$L$  = distance along heated length from start of boiling, in.

The mixture density at any point,  $\rho$ , may then be rigorously defined by

$$\rho = \frac{\alpha}{v_g} + \frac{1 - \alpha}{v_f}. \quad (\text{B-6})$$

The mixture specific volume,  $v$ , and  $\rho$  are related by

$$v = \frac{1}{\rho}. \quad (\text{B-7})$$

The frictional component of the boiling pressure drop,  $\Delta P_{fb}$ , may be expressed as

$$\Delta P_{fb} = \frac{f G^2}{2g_c D_e} \int_{L_p}^{L_h} \frac{v}{144} dL. \quad (\text{B-8})$$

From a momentum balance over the boiling length, we have

$$\Delta P_{ab} = \frac{1}{A g_c} \left[ M_b V_g + (M - M_b) V_f - M V_{fo} \right], \quad (B-9)$$

where

$V_{fo}$  = Initial liquid velocity, ft/sec,

$A$  = flow area, in.<sup>2</sup>

The static head component,  $\Delta P_{hb}$ , is given by

$$\Delta P_{hb} = \frac{g}{g_c} \int_{L_p}^{L_h} \frac{\rho}{1728} dL. \quad (B-10)$$

Combining Eqs. (B-3) through (B-10) then yields, for the frictional component,

$$\Delta P_{fb} = \frac{f G^2 v_f (L_h - L_p)}{288 g_c D_e} \left[ \frac{\frac{1}{\beta} - S}{1 - S} + \left\{ 1 - \frac{\frac{1}{\beta} - S}{1 - S} \right\} \frac{\ln \left( 1 + x_e \frac{1-S}{S} \right)}{x_e \frac{1-S}{S}} \right]; \quad (B-11)$$

for the acceleration component,

$$\Delta P_{ab} = \frac{G^2 v_f}{144 g_c} \left[ x_e \frac{\frac{1}{\beta} - S}{S} - x_e (1 - S) \left\{ 1 + x_e \frac{\frac{1}{\beta} - S}{S} \right\} \right]; \quad (B-12)$$

and for the static head component,

$$\Delta P_{eb} = \frac{g}{g_c} \cdot \frac{L_h - L_p}{1728 v_f} \left[ \frac{1 - S}{\frac{1}{\beta} - S} + \left\{ 1 - \frac{1 - S}{\frac{1}{\beta} - S} \right\} \frac{\ln \left( 1 + x_e \frac{\frac{1}{\beta} - S}{S} \right)}{x_e \frac{\frac{1}{\beta} - S}{S}} \right] .$$

(B-13)

### Overall Pressure Drop

The overall frictional component is given by

$$\Delta P_f = \Delta P_{fb} + \Delta P_{fp} , \quad (B-14)$$

and the overall acceleration component by

$$\Delta P_a = \Delta P_{ab} . \quad (B-15)$$

The overall static head component is

$$\Delta P_h = \Delta P_{hb} + \Delta P_{hp} . \quad (B-16)$$

The total pressure drop is then determined from

$$\Delta P_b = \Delta P_f + \Delta P_a + \Delta P_h , \quad (B-17)$$

which is Eq. (A-29).

Nothing has been said, thus far, about how the slip ratio, so freely used in the above equations, is to be determined. Preliminary application of the above pressure drop equations to experimental data yielded, through an iterative procedure, values of slip ratio as a

function of specific volume ratio. A log-log plot showed that, while the slope of the line through the data agreed with Zivi's<sup>25</sup> prediction, the magnitudes were substantially lower. Accordingly, a relation of the form

$$S = C \sqrt[3]{v_g/v_f} \quad (B-18)$$

was assumed and the coefficient C was determined by a "best" fit (in the least squares sense) of calculated to measured pressure drop. Figure 17 shows the resulting correlation for runs 301 through 334 of IWS data. The "best" value of C was found to be 0.16.

All the data correlate to about  $\pm 25\%$ ; note, however, that a substantial share of this scatter is ascribable to two outlying points. If these two outliers were deleted, the remaining 32 points would correlate to about  $\pm 15\%$ .

## REFERENCES

1. A. P. Fraas, et al., "A Comparative Study of Fission-Reactor-Turbine-Generator Power Sources for Space Vehicles," USAEC Report ORNL-2150, Oak Ridge National Laboratory, September 1961.
2. A. R. Barbin and M. M. Yarosh, "An Analog Study of a Single-Loop Rankine Cycle System," USAEC Report ORNL-TM-1369, Oak Ridge National Laboratory, January 1966.
3. M. M. Yarosh, "Stability and Control Characteristics of Electrically Heated Test Rigs Designed to Simulate the MPRE Fluid System," USAEC Report ORNL-TM-1370, Oak Ridge National Laboratory, January 1966.
4. R. E. MacPherson, Jr., and A. P. Fraas, "Potassium Rankine Cycle Operating Experience for the Medium Power Reactor Experiment," presented at the AIAA First Rankine Cycle Space Power Systems Specialist Conference, Cleveland, Ohio, October 1965.
5. J. Foster, "The MPRE Reactor Control Mechanism," presented at the AIAA First Rankine Cycle Space Power Systems Specialist Conference, Cleveland, Ohio, October 1965.
6. A. M. Perry, "Status of MPRE Core Design," presented at the AIAA First Rankine Cycle Space Power Systems Specialist Conference, Cleveland, Ohio, October 1965.
7. M. M. Yarosh, "Boiler Studies for the Medium Power Reactor Experiment," presented at the AIAA First Rankine Cycle Space Power Systems Specialist Conference, Cleveland, Ohio, October 1965.
8. A. P. Fraas, "Design and Development Tests of Direct-Condensing Potassium Radiators," presented at the AIAA First Rankine Cycle Space Power Systems Specialist Conference, Cleveland, Ohio, October 1965.
9. M. E. LaVerne, Space Power Program Semiannual Progress Report June 30, 1962, ORNL-3337, pp. 9-12.
10. M. E. LaVerne, "Analysis of the Hot Spot Problem in the MPRE," USAEC Report ORNL-TM-1371, Oak Ridge National Laboratory, January 1966.
11. A. P. Fraas, "Flow Stability in Heat Transfer Matrices Under Boiling Conditions," USAEC Report ORNL CF-59-11-1, Oak Ridge National Laboratory, November 1961.

12. J. W. Michel and A. M. Perry, "Design Study of Boiling Potassium Reactors for Thermal Outputs of 1 to 30 Mw," USAEC Report ORNL TM-1365, Oak Ridge National Laboratory, January 1966.
13. R. B. Korsmeyer, "Condensing Flow in Finned, Tapered Tubes," USAEC Report ORNL-TM-534, Oak Ridge National Laboratory, May 1, 1963.
14. A. P. Fraas, "Survey of Operating Conditions and Requirements for Nuclear Reactor Turbine-Generator Space Power Plants for the 1970-1985 Periods," USAEC Report ORNL-TM-1364, Oak Ridge National Laboratory, January 1966.
15. A. P. Fraas, "Effects of Power Output on Inventory and Flow Distribution through MPRE System," pp. 12-25, Space Power Program Semiann. Progr. Rept. June 30, 1963, USAEC Report ORNL-3489, Oak Ridge National Laboratory.
16. M. E. LaVerne, M. M. Yarosh, and A. R. Barbin, "System Flow Distribution, Stability, and Control," p. 13, Medium-Power Reactor Experiment Progr. Report September 30, 1963, USAEC Report ORNL-3534, Oak Ridge National Laboratory.
17. C. S. Mayo and H. D. Linhardt, Test Report of Steam-Turbine-Driven Pump, Aeronutronic Division, Ford Motor Co., March 6, 1963.
18. R. G. Cunningham, "Jet-Pump Theory and Performance with Liquids of High Viscosity," Trans. ASME, 79: 1807-1820 (1957).
19. N. C. Sher, M. S. Thesis, Univ. of Minn., Minneapolis (1955).
20. M. M. Yarosh, unpublished IWS data. (To be published.)
21. C. J. Meisl and A. Shapiro, Thermodynamic Properties of Alkali Metal Vapors and Mercury - 2nd Revision, November 9, 1960, Report R60FPD358-A, Flight Propulsion Laboratory Department, General Electric Company, Cincinnati, Ohio.
22. J. H. Keenan and F. G. Keyes, Thermodynamic Properties of Steam, 1st Ed., 1936. John Wiley and Sons, Inc., New York.
23. W. L. Owens, Jr., "Two-Phase Pressure Gradient, Paper N. 41, pp. 363-368 in Part II, Section A, International Developments in Heat Transfer, 1961 International Heat Transfer Conference, Aug. 28-Sept. 1, 1961, Boulder, Colorado.
24. V. E. Schrock and L. M. Grossman, "Forced Convection Boiling Studies," Univ. of Calif. Institute of Engineering Research Report Series, 73308 - UCX 2182, No. 2, November 1959.

25. S. M. Zivi, "Estimation of Steady-State Steam Void-Fraction by Means of the Principle of Minimum Entropy Production," Trans. ASME, Series C, Journal of Heat Transfer, 86: 247-252 (1964).



## INTERNAL DISTRIBUTION

- |       |                   |        |                                 |
|-------|-------------------|--------|---------------------------------|
| 1.    | G. M. Adamson     | 42.    | A. J. Miller                    |
| 2.    | S. E. Beall       | 43.    | A. M. Perry                     |
| 3.    | H. C. Claiborne   | 44.    | G. Samuels                      |
| 4.    | F. L. Culler      | 45.    | H. W. Savage                    |
| 5.    | J. E. Cunningham  | 46.    | A. W. Savolainen                |
| 6.    | J. H. DeVan       | 47.    | J. L. Scott                     |
| 7.    | J. Foster         | 48.    | O. L. Smith                     |
| 8-27. | A. P. Fraas       | 49.    | I. Spiewak                      |
| 28.   | A. G. Grindell    | 50.    | A. Taboada                      |
| 29.   | P. N. Haubenreich | 51.    | D. B. Trauger                   |
| 30.   | W. O. Harms       | 52.    | A. M. Weinberg                  |
| 31.   | S. I. Kaplan      | 53.    | J. R. Weir, Jr.                 |
| 32.   | P. R. Kasten      | 54.    | G. D. Whitman                   |
| 33.   | R. B. Korsmeyer   | 55.    | J. V. Wilson                    |
| 34.   | M. E. Lackey      | 56.    | M. M. Yarosh                    |
| 35.   | M. E. LaVerne     | 57.    | Gale Young                      |
| 36.   | M. I. Lundin      | 58.    | J. Zasler                       |
| 37.   | R. N. Lyon        | 59-60. | Central Research Library        |
| 38.   | H. G. MacPherson  | 61-62. | Y-12 Document Reference Section |
| 39.   | R. E. MacPherson  | 63-65. | Laboratory Records              |
| 40.   | H. C. McCurdy     | 66.    | Laboratory Records-Records Copy |
| 41.   | J. W. Michel      | 67.    | ORNL Patent Office              |

## EXTERNAL DISTRIBUTION

68. C. H. Armbruster, Wright Air Development Center, Dayton, Ohio
69. D. Blancher, Lockheed, Burbank, California
70. G. K. Dicker, AEC, Washington
71. Sherman Edwards, Lockheed, Sacramento, California
- 72-81. H. B. Finger, AEC, Washington
82. Graham Hagey, NASA, Houston
83. Carl E. Johnson, AEC, Washington
84. J. D. Lafleur, AEC, Washington
- 85-88. Bernard Lubarsky, NASA, Lewis Research Center
89. James Lynch, NASA, Washington
90. Benjamin Pinkel, Rand Corp., Santa Monica, California
91. Fred Schulman, NASA, Washington
92. Abe Silverstein, NASA, Lewis Research Center
- 93-96. R. M. Spencer, AEC, Washington
97. Jack Stearns, JPL, Pasadena, California
98. H. J. Stewart, JPL, Pasadena, California
99. G. C. Szego, IDA, Arlington, Virginia
100. T. F. Widmer, GE, Valley Forge, Philadelphia, Pennsylvania
101. Gordon Woodcock, NASA, Huntsville
102. W. Woodward, NASA, Washington

- 103-117. Division of Technical Information Extension (DTIE)
- 118. Research and Development Division, ORO
- 119-120. Reactor Division, ORO